



HAL
open science

Investigation of the different possible energy band structure configurations for planar heterojunction organic solar cells

Hind Lamkaouane, Hajar Ftouhi, Guy Louarn, Yamina Mir, Mustapha Morsli, Mohammed Addou, Linda Cattin, Jean Christian Bernède

► To cite this version:

Hind Lamkaouane, Hajar Ftouhi, Guy Louarn, Yamina Mir, Mustapha Morsli, et al.. Investigation of the different possible energy band structure configurations for planar heterojunction organic solar cells. *Solid-State Electronics*, 2022, 191, pp.108254. 10.1016/j.sse.2022.108254 . hal-03666501

HAL Id: hal-03666501

<https://hal.science/hal-03666501v1>

Submitted on 13 Jul 2022

HAL is a multi-disciplinary open access archive for the deposit and dissemination of scientific research documents, whether they are published or not. The documents may come from teaching and research institutions in France or abroad, or from public or private research centers.

L'archive ouverte pluridisciplinaire **HAL**, est destinée au dépôt et à la diffusion de documents scientifiques de niveau recherche, publiés ou non, émanant des établissements d'enseignement et de recherche français ou étrangers, des laboratoires publics ou privés.

1
2
3
4 **Investigation of the different possible energy band structure configurations for planar**
5
6 **heterojunction organic solar cells.**

7
8
9 Hind Lamkaouane^{1,4}, Hajar Ftouhi^{1,2}, Guy Louarn¹, Yamina Mir⁴, Mustapha Morsli³, Mohammed
10 Addou², Linda Cattin¹, Jean Christian Bernède^{5*}
11

12 1- Institut des Matériaux Jean Rouxel (IMN), CNRS, UMR 6502, Université de Nantes, 2 rue de la
13 Houssinière, BP 32229, 44322 Nantes cedex 3, France

14 2-Laboratoire des nanomatériaux et couches minces, FST, Université Abdelmalek Essaadi de
15 Tétouan, FST de Tanger BP 416 – Tanger, Morocco

16 3- Université de Nantes, Faculté des Sciences et des Techniques, 2 rue de la Houssinière, BP
17 92208, Nantes, F-44000 France.

18 4-Laboratoire de la Matière Condensée et des Energies Renouvelables, Faculté des Sciences et des
19 Techniques, Université Hassan II de Casablanca, B.P 5366 Maarif, Casablanca, Maroc

20 5- MOLTECH-Anjou, CNRS, UMR 6200, Université de Nantes, 2 rue de la Houssinière, BP
21 92208, Nantes, F-44000 France.
22
23
24
25
26

27 **Corresponding Author**

28
29 Jean Christian Bernède, Université de Nantes, CNRS, MOLTECH-Anjou, F-44000 Nantes, France

30 E-mail: Jean-christian.bernedede@univ-nantes.fr
31
32
33

34 **Keywords:** Solid state electronics, Planar organic photovoltaic cells, Small organic molecules,
35 Energy band structure alignments, Förster resonance energy transfer.
36
37

38 **Abstract**

39
40 We present a study of performances of organic photovoltaic cells (OPVs) using a wide variety of
41 small molecules. These OPVs use two or three molecules to form binary or ternary cells, i.e.
42 consisting of two or three flat stacked layers. Different ternary OPVs designs for efficient light
43 harvesting and energy band structure combinations are studied. Molecules have been chosen to
44 study all possible energy band structure alignments in ternary configuration. We discuss various
45 parameters limiting their efficiency, such as carrier mobility, organic layer morphology, energy
46 band structure alignment. Special attention has been paid to understand the device behavior. It is
47 shown that, if light absorption domains, carriers mobility, energy band structure alignment are
48 decisive for achieving performing OPVs, the geometry of the molecules is also decisive. In ternary
49 OPVs, the third organic layer, intercalated between the electron donor and the electron acceptor,
50 must serve as a bridge in the energy levels of the outer layers, which permits an energetic cascade
51
52
53
54
55
56
57
58
59
60
61
62
63
64
65

1
2
3
4 effect. For this effect to be positive it is necessary that this intermediate layer facilitates creation
5 and transport of charge carriers, but also that it allows transport of energy, all leading to an
6 improvement of the performance of the OPVs.
7
8
9

10 **1. Introduction**

11
12 Today, due to the need to develop renewable energies, there is a great interest in photovoltaic
13 energy. Among the different photovoltaic cells under study, due to their lightness, flexibility,
14 semi-transparency... organic cells are among the most studied [1, 2]. For efficient organic
15 photovoltaic cells (OPVs) it is necessary to use at least two organic materials, an electron donor (D)
16 and an electron acceptor (A). Two typical geometries of the active layer are possible. It may consist
17 of a blend of D and A, this configuration is called bulk heterojunction (BHJ). The second
18 possibility consists in a stacking of layers, where the active layer is made of at least two films, D/A;
19 it is called planar-heterojunction (PHJ) [3, 4]. Concretely, depending on the roughness of the
20 layers, intermediate geometries are also possible. In recent times, dramatic advances of the
21 performances of OPVs have been achieved using new promising molecules and polymers [5-7].
22 Nevertheless, the synthesis of these new materials is not trivial which means that the
23 commercialization of solar panels using them is not feasible in the near future. It is therefore
24 interesting to study the performances of cells using small molecules, although less efficient, but
25 easier to obtain with perfectly controlled synthesis and reproducible properties [8-11]. The
26 efficiency of binary OPVs, *i.e.* using two different organic materials as active layer, is limited by
27 the narrow absorption spectra of the organic materials. Ternary OPVs with two acceptor or donor
28 materials allow over-passing this limitation [12-14]. The third material, which must be ambipolar
29 (DA), can bridge the energy levels of the electron donor and the electron acceptor, which can
30 facilitate charge transport through energy cascade effect. Its light absorption must be
31 complementary to that of others organic materials present in the active layer. If these conditions are
32 fulfilled it can significantly improve the efficiency of the OPVs. However, adjusting the relative
33 thickness of the different layers and understanding the electronic processes present at their
34 interface remains a challenge. More precisely, the relative values of the highest occupied molecular
35 orbital (HOMO) and the lowest unoccupied molecular orbital (LUMO) of the organic molecules
36 used must fulfil certain rules (Supporting information Fig. S1). In a couple D/A, to obtain efficient
37 separation of the exciton charges, the offset ΔHOMO and/or ΔLUMO must be higher than the
38
39
40
41
42
43
44
45
46
47
48
49
50
51
52
53
54
55
56
57
58
59
60
61
62
63
64
65

1
2
3
4 exciton binding energy ΔExc [15-17]. Therefore, in the case of ternary OPVs, HOMO and LUMO
5 energy levels must be progressively offset in form of cascade heterojunctions, in such a way that
6 the central DA layer carries out exciton dissociation on the donor and acceptor side. Moreover, to
7 be efficient, the carrier's mobility of both types, electron and hole, of the DA must be high enough
8 to obtain an acceptable current. On the other hand, it is now well admitted that the maximum value
9 of the open circuit voltage, V_{oc} , follows the energy difference between the LUMO of A and the
10 HOMO of D (See Fig. S1). Therefore, in order to avoid any decrease of V_{oc} , in the case of ternary
11 OPV, it can be desirable to use a DA with same HOMO (or LUMO) than D (or A). Moreover, the
12 amount of light harvested by the OPV depends on the good agreement between the absorption
13 domain of the organic materials used and the solar spectrum. Prerequisites for the absorption
14 domains of organic materials, *i.e.* their band gap, the V_{oc} value and the offset ΔHOMO and/or
15 ΔLUMO value for efficient exciton charge separation make that it is necessary to determine the
16 optimum trade-off between these different values [18]. After light absorption and exciton
17 generation, two mechanisms can take place, charge transfer or energy transfer. On one hand, after
18 exciton diffusion towards an interface D/A, the exciton dissociation induces charge carriers
19 generation and then their diffusion towards the electrodes. To be efficient, in ternary OPVs, it
20 would be desirable that the excitons can be dissociated at the interfaces D/DA and DA/A. On the
21 other hand, energy transfer must be effective in addition to the charges transfer. Usually, in organic
22 material, this transfer is due to Förster resonance energy transfer (FRET), issued from coulombic
23 interaction between organic materials. This FRET is at the origin of two step exciton dissociation:
24 first, exciton diffusion by long scale FRET from D to DA, then, dissociation at interface DA/A.
25 FRET, to be efficient, needs an overlapping between the D emission spectrum and the DA
26 absorption spectrum [19-20]. This second migration route, added to the classical charge transfer,
27 allows expecting for better efficiencies for ternary OPVs compared to corresponding binary OPVs
28 [21]. All these constraints, which must be respected to obtain performing ternary OPVs, makes that
29 ternary OPVs often show limited success relative to binary OPVs. Actually, added to stresses
30 concerning band structure, carrier mobility's must be high enough, mainly in the case of the DA
31 which must be ambipolar and FRET must be possible. Moreover some difficulties due to the
32 morphology of some layers may exist due to specific grow properties of certain organic materials.
33 Nevertheless some promising results were already obtained. Therefore, in the present work, based
34 on new results and complemented by already published results, we sought to determine general
35
36
37
38
39
40
41
42
43
44
45
46
47
48
49
50
51
52
53
54
55
56
57
58
59
60
61
62
63
64
65

1
2
3
4 rules that can help us in the choice of new molecules for future performing cells. Thus we analyze
5 the results obtained with ternary cells made up of different molecules whose specific properties
6 allow exploring the effect of energy band structure, carriers mobility's, morphology... Although
7 BHI-OPVs are most often studied due to their highest efficiency, we chose the PHJ-OPV
8 configuration due to the fact that it consists in a stacking of layer, which made that it is easier to
9 discriminate between the various effects encountered and to determine the molecule from which
10 they originate. The different molecules have been chosen with sufficiently different properties in
11 order to be able to study the influence of the mobility of the carriers, of their energy band structure
12 and of their geometry. PHJ-OPVs are easy to implement by deposition under vacuum, through
13 sublimation of the small organic molecules, which provides an additional purification step. We
14 must not forget that one of the most successful companies in the field of OPVs is Heliatek which
15 realizes all of its solar panels by vacuum deposition and PHJ-OPVs appear as promising option
16 [22-23]. We show that if, as expected, the energy band structure configurations, the carriers
17 mobility, the light absorption ranges are fundamentals to achieve efficient PHJ-OPVs, the
18 geometry of the small organic molecules may be also determinant.

32 **2. Experimental**

33 **2.1 Organic molecules**

34
35 The vast majority of molecules used for this work are available on the market, only a few relatively
36 easy synthesis molecules have been made in the laboratory [24-27]. For this work,
37 CODEX-International (France) was our primary supplier. The chemical structures of the small
38 molecules are shown in supporting information, Fig. S2, while their energy diagrams are reported
39 in Fig. S3, The HOMOs and LUMOs values have been checked by cyclic measurements (S5.8). It
40 should be emphasized that the choice of molecules was guided by the fact that we wanted to study
41 all possible alignments of energy band structures (Fig. 1).

42 **2.2 Organic photovoltaic cells realization and characterization**

43
44 It is well known that if the composition of the organic active layer is primordial for performances of
45 OPVs, it is also necessary to ensure that carriers are collected after separation, which implies the
46 use of adequate electrodes with interfaces organic material/electrode efficient. Of course one of the
47 electrodes must be transparent to visible light. ITO (indium tin oxide) is the transparent electrode
48
49
50
51
52
53
54
55
56
57
58
59
60
61
62
63
64
65

1
2
3
4 the most often use due to its high conductivity and transparency. The second electrode must behave
5 like a mirror to reflect the unabsorbed light which thus passes through the layer a second time. Al is
6 often used for this purpose. To obtain efficient interfaces it is necessary to insert buffer layers
7
8
9
10 between electrodes and organic materials. From the anode side, the introduction of a thin hole
11 transporting layer (HTL) increases the work function (W_F) of ITO, which decreases the energy
12 barrier between ITO and D, W_F of ITO being around 4.7 eV, while the HOMO of D is around 5 eV
13 or more (Supporting information Fig. S1). This HTL increases significantly the OPVs
14 performance. Even if it has been shown that hybrid HTL can be highly effective, we chose in the
15 present work to used simple HTL, MoO_3 , due its simplicity which permits to improve the
16 reproducibility of the results and due to the fact that MoO_3 is well known as efficient HTL [28].
17 From the cathode side, in small molecule PHJ-OPVs, the insertion of a buffer layer called exciton
18 buffer layer (EBL), with large band gap to block excitons, improves substantially the OPV
19 efficiency. If bathocuproine is widely used as EBL, it was shown that Alq_3 allows obtaining
20 equivalent but more stable performances, so we used Alq_3 as EBL [29]. Therefore, the binary and
21 ternary PHJ-OPVs consisted of stacks according to ITO/ MoO_3 /D/A/ Alq_3 /Al and
22 ITO/ MoO_3 /D/DA/A/ Alq_3 /Al (Fig. S4), respectively. During this work C_{60} (fullerene) was the A of
23 all the ternary OPVs. SubPc (Boron subphthalocyanine chloride), which is well admitted as
24 ambipolar material [30-31], was used as DA material. As in the case of organic materials, donor or
25 acceptor character is relative, according to the respective positions of the HOMO and LUMO
26 levels, to be able to achieve all possible alignments of energy band structures we used some
27 molecules, more known as electron donors, as ambipolar layer. As a result, $AlPcCl$ (Aluminum
28 phthalocyanine chloride) was used as D or as DA, while MD2
29 (2-((5-(4(diphenylamino)phenyl)thiophen-2-yl)methylene) malononitrile) [27] and BDP
30 (tetraphenyldibenzoperiflanthene) were used as ambipolar layer. Pentacene, M8-1
31 ((E)-2-cyano-3-(5-((E)-2-(9,9-diethyl-7-(methyl(phenyl)amino)-9H
32 -fluoren-2-yl)vinyl)thiophen-2-yl)acrylic acid) [26], $CuPc$ (Copper phthalocyanine), BSTV
33 ((E)-bis-1,2-(5,5''-Dimethyl-(2,2':3',2''-terthiophene)vinylene) [25] and 5T (Pentathiophene)
34 [24] were used as D (Fig. 1).

35
36
37
38
39
40
41
42
43
44
45
46
47
48
49
50
51
52
53
54
55
56
57
58
59
60
61
62
63
64
65
The manufacturing of binary and ternary PHJ-OPVs, previously described in other publications, is quickly recalled in the supporting information S4. In the same way, the characterization techniques used during this work are presented in the supplementary information S5 [24-25].

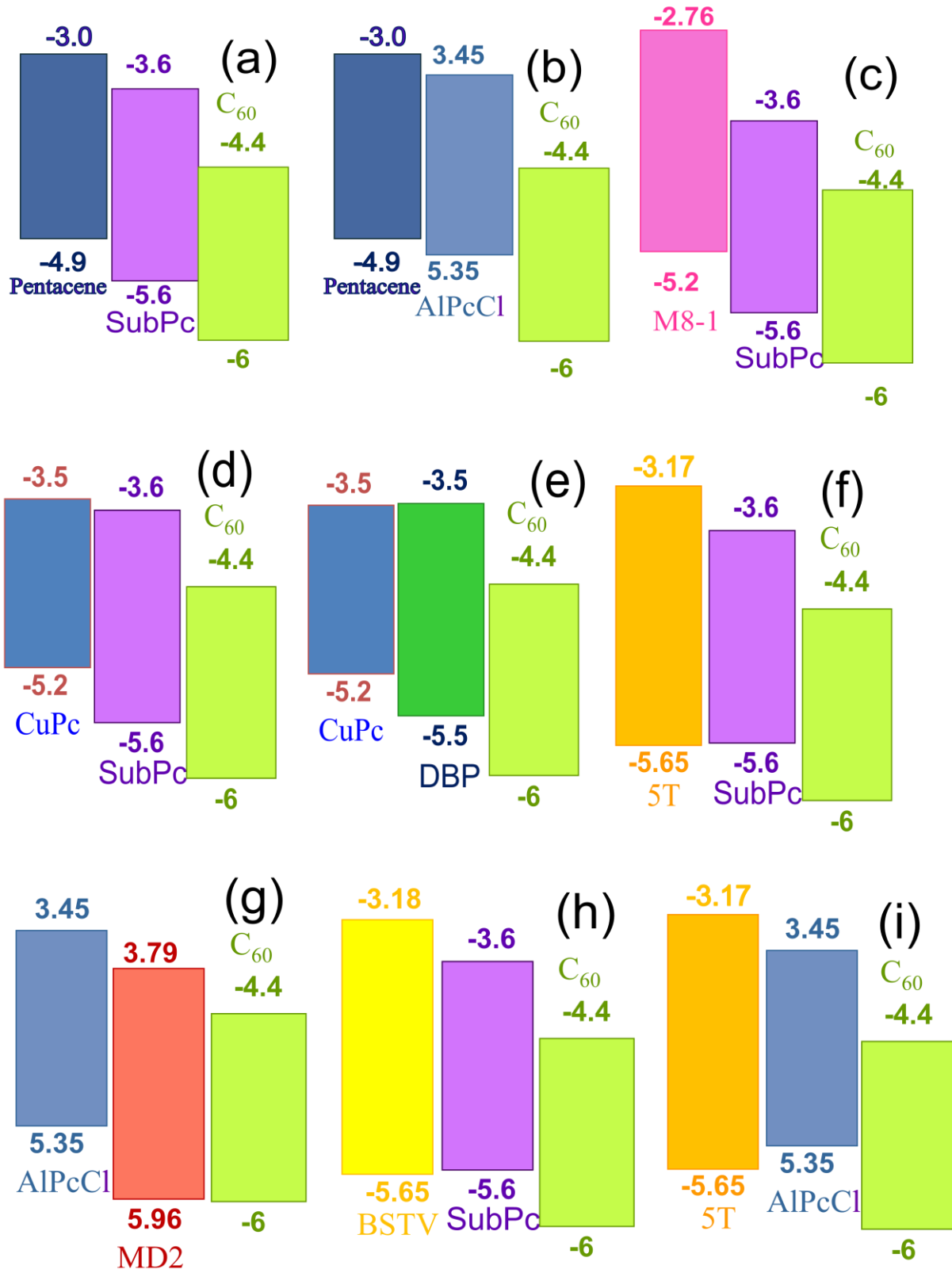


Figure 1. Energy levels alignments for the different ternary OPVs configurations studied.

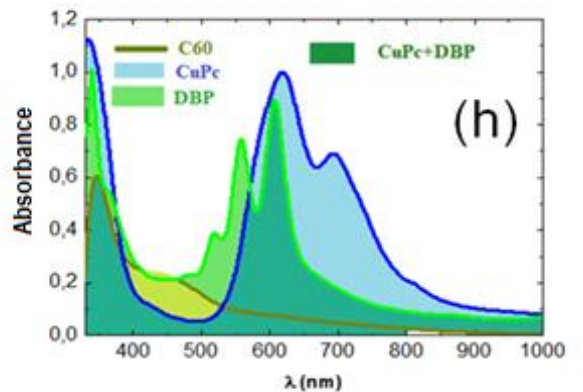
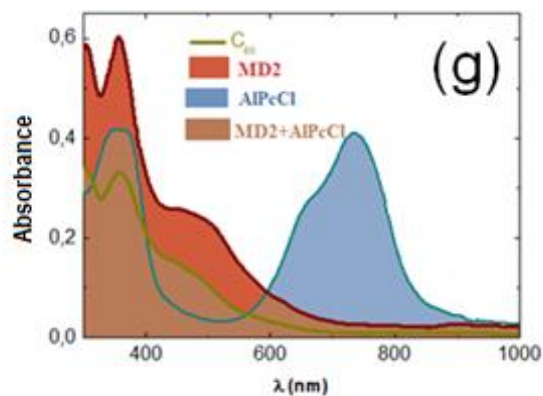
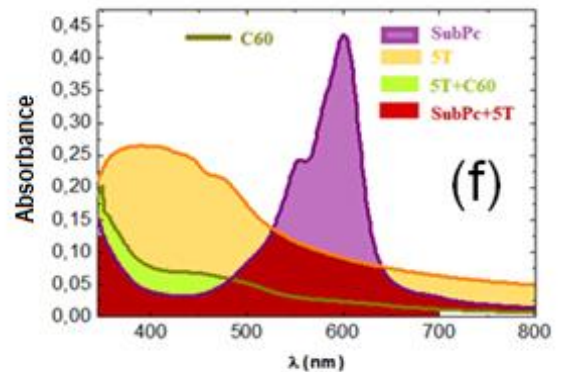
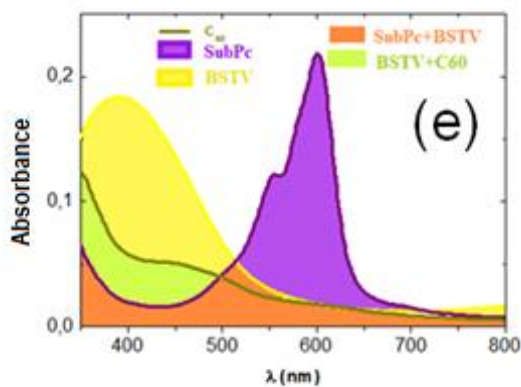
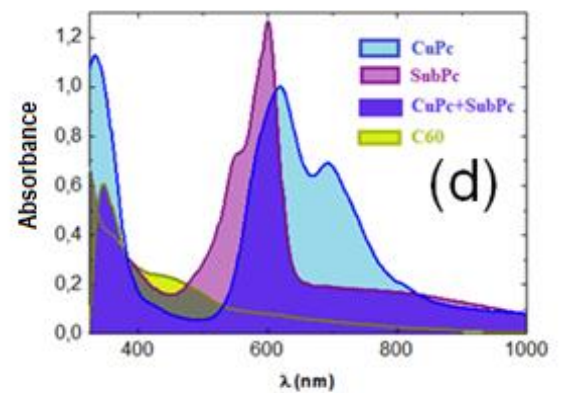
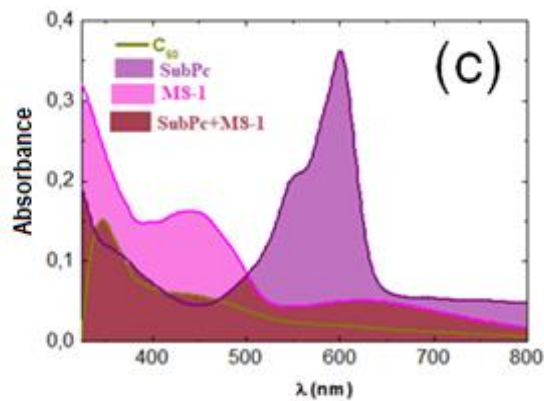
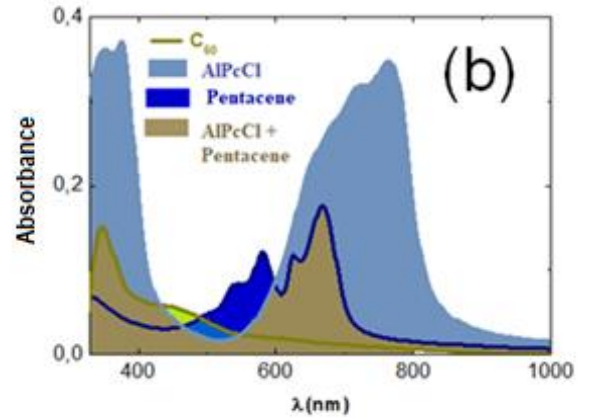
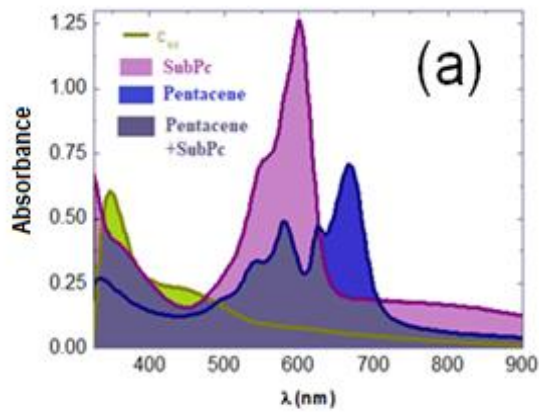
3. Results

The idea of present work was to realize and study all possible combinations of alignment of energy band structure in ternary OPVs. All of these configurations are shown in Fig. 1.

They are presented in a specific order, first the classical “ideal” energy cascade structures (Fig. 1a-c), then the structures having two components of the same LUMO (Fig. 1d, e), then those having two same HOMO (Fig. 1f-h), finally a last unconventional configuration (Fig. 1i). To refine this study, some energy band structure configurations have been repeated but using molecules with different properties such as carrier mobility, photoluminescence or morphology of layers. Thereby, some configurations are similar but with different molecules which allows to see that parameters, such as carrier mobility, layer morphology..., others than the energy band structure configuration are determinant. The UV-vis absorption spectra of the nine ternary PHJs of Fig. 1 are shown in Fig. 2. It can be seen that all the configurations result in a significant widening of the absorption domain.

We present firstly the study of the ternary OPV using CuPc as D, SubPc as DA and C₆₀ as A (Fig. 1d), due to the fact that they are often chosen as active molecules in PHJ-OPV. The goal of the purpose of producing ternary OPVs was to surpass the efficiencies obtained with binary OPVs, thus we compare the results obtained with the couples CuPc/C₆₀, SubPc/C₆₀ and CuPc/SubPc with those obtained with the ternary OPV CuPc/SubPc/C₆₀. The results, obtained after optimisation, are presented in Fig. 3 and are summarized in Table 1. The optimisation of the OPV performances through the variation of the thickness of the different layers is presented in supporting information S6 (Table S6).

1
2
3
4
5
6
7
8
9
10
11
12
13
14
15
16
17
18
19
20
21
22
23
24
25
26
27
28
29
30
31
32
33
34
35
36
37
38
39
40
41
42
43
44
45
46
47
48
49
50
51
52
53
54
55
56
57
58
59
60
61
62
63
64
65



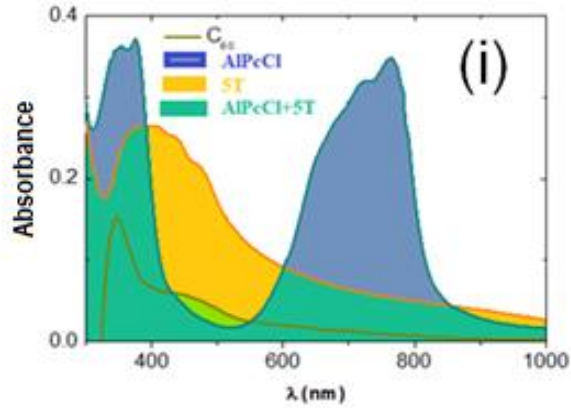


Figure 2. UV-vis absorption spectra of the nine ternary PHJs of Figure 1.

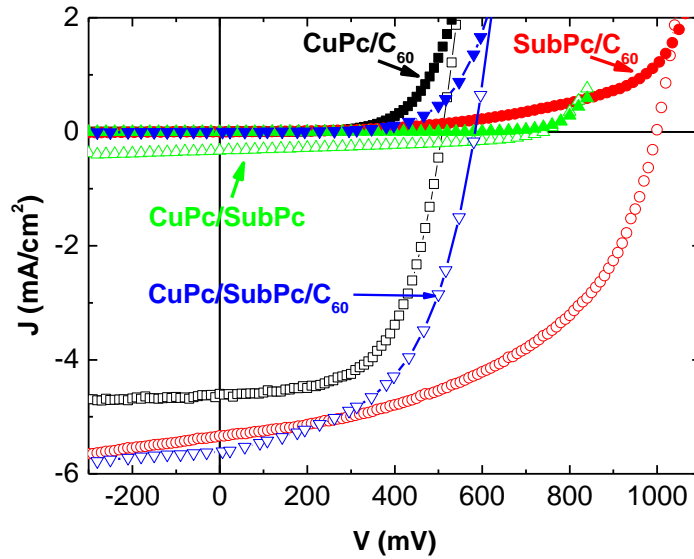


Figure 3. J-V characteristics of binary and ternary OPVs: ITO/MoO₃/active layers/Alq₃/Al, the active layer being CuPc/C₆₀ (■), SubPc/C₆₀ (●), CuPc/SubPc (▲) and CuPc/SubPc/C₆₀ (▼), (the filled symbols correspond to dark conditions while the open symbols correspond to light AM 1.5 conditions).

Table 1. Parameters of the OPV family using CuPc, SubPc and C₆₀.

Active layer (thickness-nm)	Voc (V)	Jsc (mA cm ⁻²)	FF (%)	η (%)
CuPc (30)/C ₆₀ (40)	0.50	4.68	60	1.42
SubPc (20)/C ₆₀ (40)	1.00	5.33	50	2.63
CuPc (30)/SubPc (15)	0.74	0.33	41	0.09
CuPc (30)/SubPc (15) ^{a)}	0.75	0.48	33	0.12
CuPc (30)/SubPc (15)/C ₆₀ (40)	0.58	5.54	55	1.77

^{a)} HTL MoO₃/CuI and not MoO₃ alone.

The optimum efficiency of the ternary OPV, CuPc/SubPc/C₆₀ is only 1.77%, which is higher than that of the binary OPV based on CuPc/C₆₀, but smaller than that of SubPc/C₆₀. On one hand, the short circuit current, Jsc, of the ternary OPV, overpass that of all the binary OPVs of the family, which was expected since, as visible in Fig. 2d, the insertion of SubPc between CuPc and C₆₀ widen the absorption domain of the OPV. Unfortunately, on the other hand, as predicted by the theoretical maximum value of the open circuit voltage (Fig. S1 and Fig. 1d), Voc, of the ternary OPV far is smaller than that of the couple SubPc/C₆₀. Moreover, the success of the attempt to improve the efficiency of the OPVs by moving from 2 to 3 layers in the active organic layer also depends on the efficiency of the D/DA and DA/A interfaces. Fig. 3 and Table 1 show that the binary OPV based on CuPc/SubPc underperforms with very small Jsc and small Fill Factor (FF). In order to check the activity of the interface CuPc/SubPc we proceeded to External Quantum Efficiency (EQE) (see S5.2).

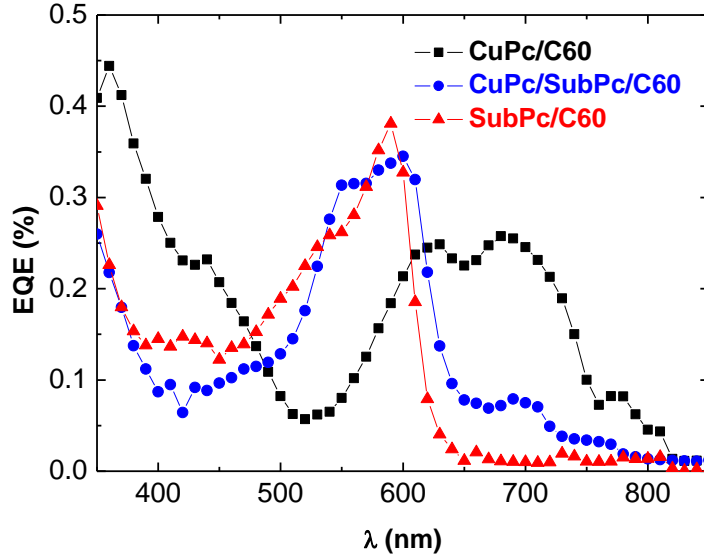


Figure 4. EQE spectra of OPV with different active layers: (■) CuPc/C₆₀, (▲) SuPc/C₆₀ and (●) CuPc/SubPc/C₆₀.

First of all, it must be noted that we were unable to measure the EQE spectrum of the OPVs based on the couple CuPc/SubPc, the photocurrent being too small. In the Fig. 4, the EQE spectra, in the case of CuPc/C₆₀ and SubPc/C₆₀ reproduce clearly the absorption spectra of CuPc and SubPc respectively (Fig. 2d), with a small contribution of C₆₀. On the contrary, the shape of the EQE spectrum of the CuPc/SubPc/C₆₀ active layer is quite different from the light absorption of these superposed three layers. In fact, the shape of the EQE spectrum is similar to that of SubPc/C₆₀. It means that the main contribution to the photocurrent in the ternary cell is due to the couple SubPc/C₆₀, with a very small contribution of CuPc between 650 nm and 750 nm. It can be concluded from the electrical study that the contribution of CuPc to the photocurrent is very small, which explains that the efficiency of the ternary OPV is smaller than that of the binary OPV based on the SubPc/C₆₀ couple.

On the other hand, it is known that, when deposited by sublimation under vacuum, the films of CuPc are crystallized. Usually, the CuPc molecules are perpendicular to the plan of the substrate. Nevertheless, when specific substrates, such as CuI, are used, the molecules are parallel to the substrate [32]. Generally, the organic molecule layers are amorphous. It is possible that the crystallized surface of CuPc layers disturbs the interface CuPc/organic layer according to the

1
2
3
4 orientation of the CuPc molecules. Moreover, it is important to note that the energy level of the
5 small molecules strongly depends on the molecular orientation. For instance, in the case of CuPc,
6 it has been shown that the value of the HOMO depends on this orientation [33]. In absolute value
7 it is 4.75 eV for the standing-up CuPc and 5.15 eV when the molecules are the parallel to the
8 substrate. Therefore, since when deposited onto MoO₃ the CuPc are perpendicular to the plan of
9 the substrate while they are parallel when they are deposited onto CuI, we have studied the
10 properties of ITO/MoO₃/CuI/CuPc/SubPc/Alq₃/Al OPVs. Unfortunately, as shown in Table 1, the
11 results are similar to those obtained with MoO₃ alone as HTL. It means that the failure of the
12 CuPc/SubPc interface is not related to the orientation of the CuPc molecules.
13

14
15 We have verified another possibility of trouble. The band gap of SubPc is significantly wider
16 than that of CuPc. Therefore, since in the classical configuration, the light crosses first the CuPc
17 layer, it may penalize the light harvesting by SubPc. So, we have checked this possible trouble by
18 probing inverted OPVs. In inverted OPVs, the ITO is used as a cathode, which corresponds
19 presently to OPVs such as ITO/Alq₃/SubPc/CuPc/MoO₃/Al, so that the light crosses SubPc
20 before CuPc, *i.e.* large band gap material before small band gap. Unfortunately, the results
21 obtained are even worse than those obtained with classical OPVs (supporting information Table
22 S6). Actually, this result is in good agreement with the EQE spectrum of the ternary OPV which
23 shows that the main contribution to the photocurrent is due to SubPc, which means that its
24 interaction with light was not penalized by the fact that CuPc was crossed by light before SubPc
25 itself.
26

27
28 In order to explain the inefficiency of the interface CuPc/SubPc, we had to investigate the specific
29 properties of these materials which may be involved in their electronic exchanges: charge carriers
30 mobility's, surface roughness, optical density, photoluminescence. As it will be interesting to know
31 these properties for the other molecules used during this work we have proceeded to a systematic
32 experimental study of these for all the molecules concerned. We draw up a balance table of the
33 properties of the different materials used.
34
35
36
37
38
39
40
41
42
43
44
45
46
47
48
49
50
51
52
53
54
55
56
57
58
59
60
61
62
63
64
65

Table 2. Diverse parameters of the organic layers used.

Molecule	μ_{e^-} ($\text{cm}^2 \text{v}^{-1} \text{s}^{-1}$)	μ_h ($\text{cm}^2 \text{v}^{-1} \text{s}^{-1}$)	RMS ^{b)} (nm)	O. D. Absorption range (nm)	PL ^{c)} Emission range (nm)
Pentacene	-	$7.5 \cdot 10^{-3}$	4-7	500-700	660-700 ; 730-950
CuPc	$5.8 \cdot 10^{-3}$	$1.1 \cdot 10^{-3 \text{ a)}$	3	550-800 ; 300-400	1075-1175
M8-1	$1.6 \cdot 10^{-9}$	$6 \cdot 10^{-7}$	3.5	530-580 ; 300-530	525-750
BSTV	-	$9.5 \cdot 10^{-6}$	1.55	350-500	500-650
5T	-	$1.7 \cdot 10^{-4}$	18	350-600	475-625
AlPcCl	$6.9 \cdot 10^{-4}$	$4 \cdot 10^{-5}$	6	800-600 ; 400-300	660-720 ; (770)
DBP	$1.6 \cdot 10^{-4}$	$2 \cdot 10^{-4}$	-	500-650 ; 300-450	-
SubPc	$8 \cdot 10^{-3}$	$1.7 \cdot 10^{-5}$	-	500-650 ; 430-300	-
MD2	$1.5-3 \cdot 10^{-7}$	$1 \cdot 10^{-5}$	-	500-300	-

a) When deposited onto CuI the hole mobility of CuPc is $2 \cdot 10^{-3} \text{ cm}^2 \text{v}^{-1} \text{s}^{-1}$

b) Values measured for the organic bottom layer D.

c) From luminescence spectra shown in Fig. S7 or extracted from the bibliography: 5T [35], Pentacene [38], AlPcCl [39], and CuPc [40].

Thus, in Table 2 the electron and hole mobility of the different molecules are enumerated. The values reported have been measured using the space charge limited current technique (SCLC; Supporting information S5.3). The experimental values are of the same order of magnitude than those found in the literature, for instance $2 \cdot 10^{-4} \text{ cm}^2 \text{v}^{-1} \text{s}^{-1}$ for the hole mobility of DBP to be compared to $1 \cdot 10^{-4} \text{ cm}^2 \text{v}^{-1} \text{s}^{-1}$ encountered in earlier publication [34] and $7.5 \cdot 10^{-3} \text{ cm}^2 \text{v}^{-1} \text{s}^{-1}$ Pentacene, what is, as expected, the highest mobility measured (Table 2) [35]. About CuPc, if better results were published, $2.1 \cdot 10^{-2} \text{ cm}^2 \text{v}^{-1} \text{s}^{-1}$, [36], the measured value, $2 \cdot 10^{-3} \text{ cm}^2 \text{v}^{-1} \text{s}^{-1}$ is situated in the range of purified CuPc according to Rhonda F. Salzman et al. [37].

In addition, it is known that in PHJ-OPV the roughness of the bottom organic layer, when too high, may induce leakage currents which results in Voc and FF decrease, so the root mean square (RMS) roughness is noted in the Table 2. In the same way, we have seen that FRET, to be efficient, needs a clear overlapping between the D photoluminescent spectrum (PL) and absorption spectrum of the DA layer, so the PL domain of the D layer and the absorption domain of the DA layer are schematically reported in Table 2.

1
2
3
4 About the couple CuPc/SubPc, the Table 2 shows that μ_h of CuPc is among the highest of the
5
6 Table, while the μ_e of SubPc is high enough to use it as ambipolar material. Also, the RMS of
7
8 CuPc is of the same order of magnitude as that measured for most D layers. Nevertheless, there is
9
10 no overlapping between the PL spectrum of CuPc and the absorption of SubPc, which makes that
11
12 energy transfer (FRET) appears improbable, which may be a start to explaining the poor results
13
14 obtained.

15 In order to look more carefully for the origin of the trouble we have substituted DBP to SubPc.
16
17 As shown in Fig. 1 the band scheme d and e are nearly similar. The obtained results are
18
19 summarized in Table 3.
20
21

22 Table 3. Parameters of the OPV family using CuPc, DBP and C₆₀.
23
24

Active layer (thickness-nm)	Voc (V)	Jsc (mA cm ⁻²)	FF (%)	η (%)
DBP (20)/C ₆₀ (40)	0.76	3.01	38	0.88
CuPc (30)/C ₆₀ (40)	0.50	4.68	60	1.42
CuPc (30)/DBP (15)	0.24	1.02	25	0.06
CuPc (30)/DBP (10)/C ₆₀ (40)	0.30	1.59	40	0.20

25
26
27
28
29
30
31
32
33
34
35
36
37 It can be seen that the result are worst than those obtained with SubPc. Nevertheless, the electron
38
39 mobility of DBP, $\mu_e = 1.6 \cdot 10^{-4} \text{ cm}^2 \text{ v}^{-1} \text{ s}^{-1}$ (Table 2), if not very high, is not so bad and cannot
40
41 justify the very bad performance of the OPV based on the couple CuPc/DBP. However, one can
42
43 see in table 2 that, here also, there is no overlapping between the PL spectrum of CuPc and the
44
45 absorption of DBP.

46 In front of these results, we propose possible hypotheses of interpretation.
47

48 About the ternary PHJ-OPVs with CuPc as donor, it appears that, whatever the ambipolar layer,
49
50 SubPc or DBP, there is no overlapping between the PL spectrum of CuPc and the absorption
51
52 range of the DA layer. About the PL spectrum of CuPc Chuan-Hui Cheng et al. measured a small
53
54 near-infrared electrophosphorescence at 1.1 μm [40]. Even if the PL signal is small, others
55
56 studies confirm that the emission range of CuPc is around 1.1 μm [41, 42]. It can be concluded
57
58 that there is no overlapping between the PL spectrum of CuPc and the absorbance of SubPc or
59
60 DBP, which excludes the possibility of energy transfer (FRET) from CuPc to the central
61
62
63
64
65

1
2
3
4 ambipolar layer. Such absence can explain the disappointing results obtained with the ternary
5 PHJ-OPVs CuPc/SubPc/C₆₀ and CuPc/DBP/C₆₀. Similarly, it was shown that, while there was an
6 efficient energy transfer (FRET) from P3HT to C₆₀ via TPD (N,N'-diphenyl-N,N'—bis
7 (3-methylphenyl)[1,1'-bisphenyl]-4,4'-diamine), there is not in the case of CuPc/TPD/C₆₀
8 devices, which was attributed to the fact that FRET is a function of the photoluminescence
9 quantum yield of D and the degree of overlap between the A absorption spectrum and the D
10 emission spectrum [43].
11

12
13
14
15
16
17 On the other hand, it must be noted that the CuPc molecules are plane and their films are
18 crystallized, while those of SubPc (Fig. S2) and DBP (See Fig. S8.1) are not plane and their films
19 are amorphous. Such differences in structures can lead to some disorder at the interface and
20 consequently poor interface properties. Actually, it is well known for a long time that PTCBI, in
21 the same way that C₆₀, allows obtaining efficient OPVs based on the couple CuPc/PTCBI [44]
22 and it turns out that the PTCBI molecules are plane. In fact perylene molecules such as PTCBI,
23 PTCDA, PTCDI-C₇H₁₅ are plane as shown in supporting information Fig. S8.2. To explore this
24 hypothesis, we have probed binary OPVs based on couple CuPc/perylene. It can be seen in
25 supporting information S9 (Table S9 and Fig. S9) that all the couples probed, CuPc/PTCBI,
26 CuPc/PTCDI-C₇H₁₅ and CuPc/PTCDA give far better results than those obtained with the
27 couples CuPc/SubPc or CuPc/DBP, even in the case of PTCDA despite its small carrier mobility.
28 These results reinforce our hypothesis regarding the possible influence of molecular geometry on
29 cells performance, via the activity, or not, of the interface donor/acceptor.
30

31
32 In order to achieve more information about the effect of the CuPc/A (C₆₀ or SubPc) interface on
33 the PHJ-OPV performances, we proceeded to deeper analysis of the J–V characteristics of the
34 binary OPVs based on CuPc/C₆₀ and CuPc/SubPc. The variation of the photocurrent density, J_{ph},
35 with the effective voltage, V_{eff}, has been studied with:
36
37

$$38 \quad J_{ph} = J_L - J_D \quad (1)$$

$$39 \quad V_{eff} = V_0 - V_a \quad (2)$$

40
41 where J_L is the current density under AM 1.5 light, J_D is the current density in dark and V₀
42 corresponds to the voltage when J_{ph} is equal to zero, while V_a is the applied voltage. It can be
43 seen in Fig. 5 that, if, as expected [12], a saturation state is achieved at about 1 V in the case of
44 the OPV with CuPc/C₆₀ as active layer, there is no visible tendency to saturation in the case of
45 OPV with CuPc/SubPc. The absence of visible saturation in this last case indicates that there is
46
47
48
49
50
51
52
53
54
55
56
57
58
59
60
61
62
63
64
65

high recombination loss at the interface CuPc/subPc which confirms the bad properties of this interface.

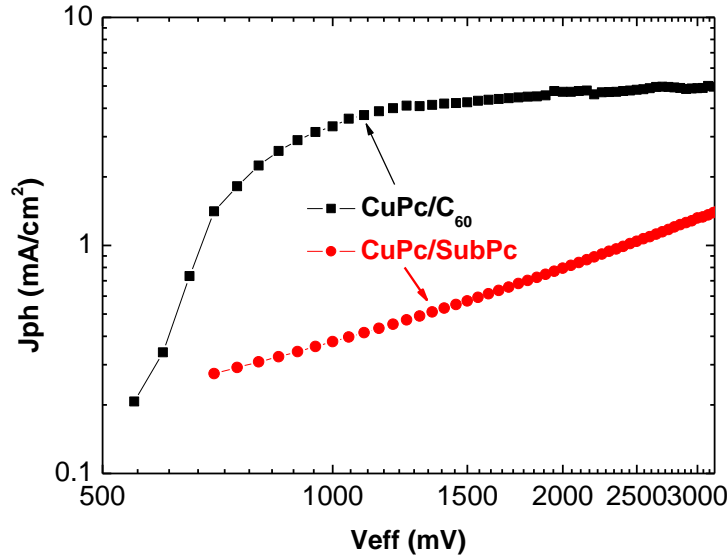


Figure 5. J_{ph} - V_{eff} curves of OPVs with different active layers (■) CuPc/C₆₀ and (●) CuPc/SubPc.

Therefore, the absence of transfer energy (FRET) and the bad interface properties due, possibly, to poor geometrical compatibility, explain, the limited performances of the PHJ-OPVs using CuPc as donor when coupled with SubPc or DBP.

In order to pursue the investigation of the effect of energy band structure configurations on the performances of PHJ-OPVs, we have studied cascade energy levels configuration, such as those corresponding to Fig. 1a,b,c. When Pentacene is used as D, its high electron mobility allows using quite thick layer (60 nm). This allows more light to be absorbed which results in a higher photocurrent. Unfortunately, as shown in Fig. 1a, b, the energy difference between the HOMO of pentacene and the LUMO of C₆₀ is small, which limits drastically the Voc value (Fig. S1) [45]. For instance, in the case of the Pentacene, SubPc and C₆₀ family, for the ternary OPV (Pentacene (60nm)/SubPc (15nm)/C₆₀ (40nm)), the efficiency is limited to 2.90%, while Jsc is 12.40 mA cm⁻² and FF = 51%, due to the fact that Voc is only 0.46 V. In the same way, if we substitute AlPcCl to SubPc, the maximum efficiency of the pentacene (60nm)/AlPcCl (15nm)/C₆₀ (40nm) ternary OPV is 2.05%, with Jsc = 12 mA cm⁻², FF = 47%, but Voc = 0.37 V. By comparison with the Voc of SubPc/C₆₀ or AlPcCl/C₆₀ which are 1V and 0.70 V respectively, it is clear that, due to

1
2
3
4 its HOMO value, -4.9 eV, the efficiency of the OPVs using Pentacene is significantly penalized.
5
6 Nevertheless, the shape of the EQE spectra of the ternary OPVs pentacene/SubPc/C₆₀ and
7
8 Pentacene/AIPcCl/C₆₀ (See S10) follow the corresponding optical density spectra (Fig. 2a, b).
9
10 Clearly the three organic molecules of each OPV contribute to the photocurrent (Fig. S10) and it
11
12 can be said that, contrarily to the case of CuPc/SubPc/C₆₀, both interfaces D/DA and DA/A are
13
14 active. This justifies that the efficiency of the ternary OPVs is higher, at least slightly, than that of
15
16 the corresponding binary OPVs, only by 0.5% in the case of pentacene/AIPcCl/C₆₀, but 10% in
17
18 the case of Pentacene/SubPc/C₆₀. Nevertheless, as said above, the performances are limited by
19
20 the HOMO of pentacene. Actually, the third cascade structure of Fig. 1d, allows us to confirm
21
22 the effect of the HOMO value on the Voc value. Due to its HOMO at -5.2 eV, M8-1, in the
23
24 M8-1/SubPc/C₆₀ ternary OPV, permits achieving a Voc of 0.73 eV, which corroborates the fact
25
26 that the Voc value increases with $\Delta(\text{LUMO}_A\text{-HOMO}_D)$. Sadly, the hole mobility of M8-1 is very
27
28 small (Table 2) and the resulting OPV efficiency is limited to 0.8%.

29
30 The maximum theoretical value of Voc is equal to the difference between the LUMO of A and
31
32 the HOMO of D. Therefore, in the case of ternary cells, to avoid a loss in the value of Voc, it can
33
34 be desirable to use materials of which two of them have the same HOMO or LUMO. Since the
35
36 results obtained by using D and DA with same LUMO (Fig. 1d and 1e) were disappointing, we
37
38 decided to probe ternary OPVs using D and DA with the same HOMO value, BSTV/SubPc/C₆₀
39
40 (Fig. 1h) and 5T/SubPc/C₆₀ (Fig. 1f). The Fig. 1 shows that both ternary structures exhibit the
41
42 same energy band structure, the main difference consists in the higher hole mobility of 5T
43
44 compared to that of BSTV (Table 2). A previous study, but with a different HTL, has already
45
46 shown that very good results can be achieved with BSTV [46], which is not the case with 5T
47
48 [47]. Nevertheless, to increase the reliability of the comparison of the results obtained, we
49
50 repeated the study, each of the molecules being from the same batch. Moreover, for simplicity,
51
52 we used a simple HTL, MoO₃ alone and not MoO₃/CuI. The results reinforce, those obtained
53
54 previously, namely with an increase in efficiency of 20 % in the case of the ternary OPV using
55
56 the BSTV as D (Fig. 6).
57
58
59
60
61
62
63
64
65

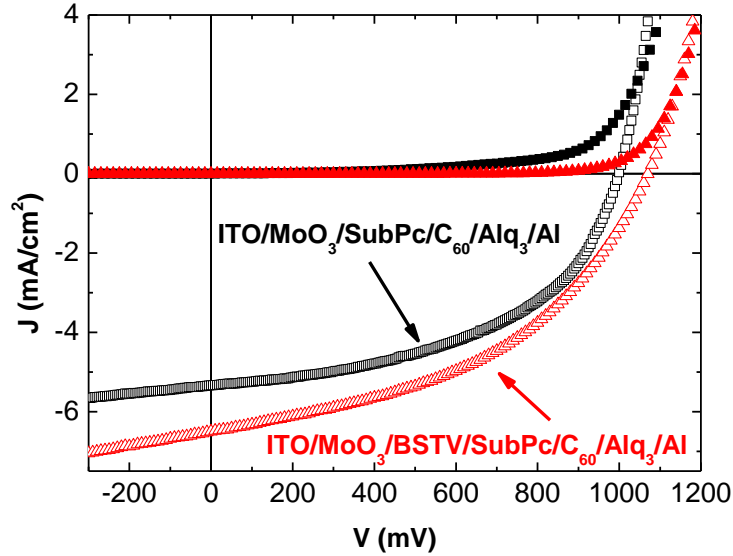


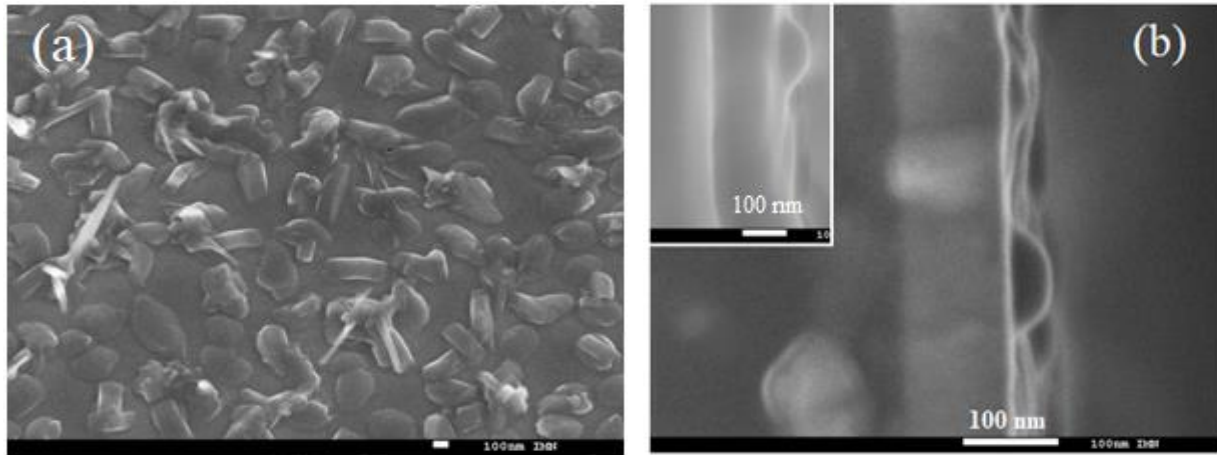
Figure 6. J - V characteristics of binary and ternary OPVs: ITO/MoO₃/active layers/Alq₃/Al, the active layer being SubPc/C₆₀ (■), BSTV/SubPc/C₆₀ (●), (the filled symbols correspond to dark conditions while the open symbols correspond to light AM 1.5 conditions).

The parameter of the champion OPV (BSTV (16 nm)/SubPc (12.5)/C₆₀ (40nm)) are $V_{oc} = 1.07$ V, $J_{sc} = 6.6$ mA cm⁻², FF = 45% and $\eta = 3.14\%$ to compare with the parameters of the binary OPV SubPc/C₆₀ in Table 1. This good result can be associated to the fact that the Förster resonance energy transfer from the BSTV layer to the SubPc layer is highly probable since the PL spectrum of BSTV (Fig. S7.2) overlaps the absorption spectrum of SubPc (Fig. 2, Table 2). Moreover, the hole mobility of BSTV is of the same order of magnitude than that of SubPc (Table 2), while the absorption range of both molecules are complementary (Fig. 2e).

As regards 5T, which HOMO and LUMO values are similar to those of BSTV, unexpectedly, while its hole mobility is higher than that of BSTV, the obtained performances were very poor. In the case of ITO/MoO₃/CuI/5T/SubPc/C₆₀/Alq₃/Al ternary OPV, the maximum efficiency achieved was only 0.80%, to compare with the 0.81% obtained with the couple 5T/C₆₀. This disappointing result was correlated to the small V_{oc} value, 0.38 V, while in the case of BSTV/SubPc/C₆₀, $V_{oc} = 1.07$ V. It was shown that this small V_{oc} value was due to the too high surface roughness of the 5T layer, high RMS which induces high leakage current and therefore small V_{oc} value [47]. In fact, about the effect of the roughness of organic material interface, two

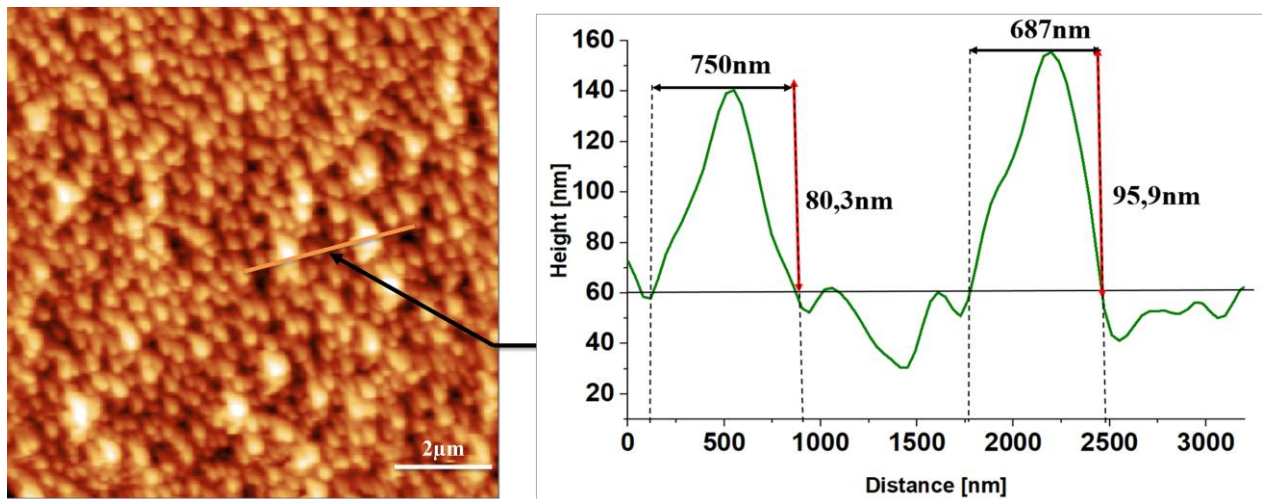
1
2
3
4 contradictory effects occur. The first effect is positive, as said by Kjell Cnops et al [48], the high
5 surface roughness of the underlying donor layer increases the interface area compared with the
6 projected area, which permits most excitons generated in the acceptor layer to reach the D/A
7 interface, resulting in high J_{sc} values. On the other hand, the second effect is due to the fact that,
8 a too high roughness induces leakage currents, which results in a decrease of V_{oc} and FF [49].
9 For instance, as shown below, in the case of 5T layers, the maximum height of the peak-to-valley
10 (PV) profile is of the same order of magnitude than the whole organic active layer (Fig. 8). Such
11 high roughness induces shunt paths, which may induce some performance limitation via an
12 increase in the leakage current. Therefore, increase in interface roughness improves J_{sc} through
13 the increase the interface area D/A, but it decreases the V_{oc} and FF value through leakage
14 currents and it is necessary to determine the optimum trade-off between these different effects. In
15 the present case of 5T, it appears that the negative effect of induced leakage current overpass
16 largely the positive effect of the interface area increase. Nevertheless, as shown in the case of
17 CuPc for instance, it is known that CuI modifies strongly the morphology of the organic layer
18 which is deposited on it. Therefore, to circumvent the effect of CuI as template, the 5T layers
19 were deposited onto MoO_3 HTL layer and not as previously on MoO_3/CuI . Nevertheless, as
20 shown by the SEM study, a high density of grains is visible at the surface of the 5T layer
21 deposited onto MoO_3 (Fig. 7a). Some grains seem nearly perpendicular to the substrate, what is
22 confirmed by the cross-section shown in Fig. 7b. The inset in Fig. 7b corresponds to the cross
23 section of a 5T layer deposited onto MoO_3/CuI . The grain visible in this inset is similar to that
24 visible in the 5T film deposited onto MoO_3 . This shows that the roughness of the 5T layers is
25 more or less similar whether the layer is deposited on MoO_3 or MoO_3/CuI . This hypothesis is
26 comforted by the AFM study. In Fig. 8, we can see an AFM image, $10\ \mu m \times 10\ \mu m$, of a 5T layer
27 deposited on ITO/ MoO_3 . The RMS deduced from this image is 18 nm. Even if this RMS is
28 smaller than that obtained when 5T is deposited on ITO/ MoO_3/CuI (30 nm), it stays far higher
29 than the value encountered in the case of the others D (Table 2). Moreover, some high features
30 are visible at the surface of the ITO/ MoO_3 anode. As shown by the profile issued from the AFM
31 image, these features are as high as 90 nm, which means that they are nearly as thick as the whole
32 PHJ-OPV cell. Actually, it can be seen in Fig. S11 that the leakage current in the case of the
33 ternary OPV 5T/SubPc/ C_{60} is far higher than that measured in the case of BSTV/SubPc/ C_{60} ,
34 which justifies the measured large difference in V_{oc} values, 0.38 V with 5T and 1.07 V with
35
36
37
38
39
40
41
42
43
44
45
46
47
48
49
50
51
52
53
54
55
56
57
58
59
60
61
62
63
64
65

1
2
3
4 BSTV, while they have similar band scheme configurations. Therefore, the surface of the anode
5 being too rough, large leakage currents is obtained. It follows that, the same causes having the
6 same effects, the performances of the OPVs based on 5T/SubPc/C₆₀ are limited due to the small
7 Voc value obtained, whatever the HTL, MoO₃/CuI or MoO₃.
8
9
10



28
29 Figure 7. (a) Surface visualization of a 5T layer deposited on MoO₃; (b) Cross section of a
30 structure glass/ITO/MoO₃/5T.

31
32
33 Inset Figure 7b. Cross section of a structure glass/ITO/MoO₃/CuI/5T.



53
54 Figure 8. AFM image of a 5T layer and profile of the image following the visualized line.

55
56 As part of the study of the effect of the energy band structure alignment on the performances the
57 PHJ-OPVs structure, where DA and A have the same HOMO have been studied, through
58 AIPcCl/MD₂/C₆₀ PHJ-OPVs (Fig. 1g) [47].
59
60
61
62
63
64
65

Here DA and A have the same HOMO whereas in the previous case it was D and DA. The results obtained in a recent study show that this configuration works. However, for the case studied the electron mobility of DA limits the obtained results [47].

There remains a last case for which the configuration is unfavorable to the proper functioning of the PHJ-OPV (Fig. 1i). This study was conducted using the ternary OPV, 5T/AIPcCl/C₆₀. If limited to the case where the intermediate layer is thick enough to be continuous (18 nm) [47], the performance for the 5T/AIPcCl/C₆₀ is poor, with a maximum energy conversion efficiency of 0.7%. To explain this small efficiency we have focused our interest to the behavior of the 5T/AIPcCl couple. The optimum efficiency of the corresponding OPV, with 70 nm of 5T and 22 nm of AIPcCl, is $\eta = 0.46\%$ with $V_{oc} = 0.40$ V, $J_{sc} = 2.95$ mA cm⁻² and 39% as FF. The EQE spectrum of this binary OPV is shown in Fig. 9.

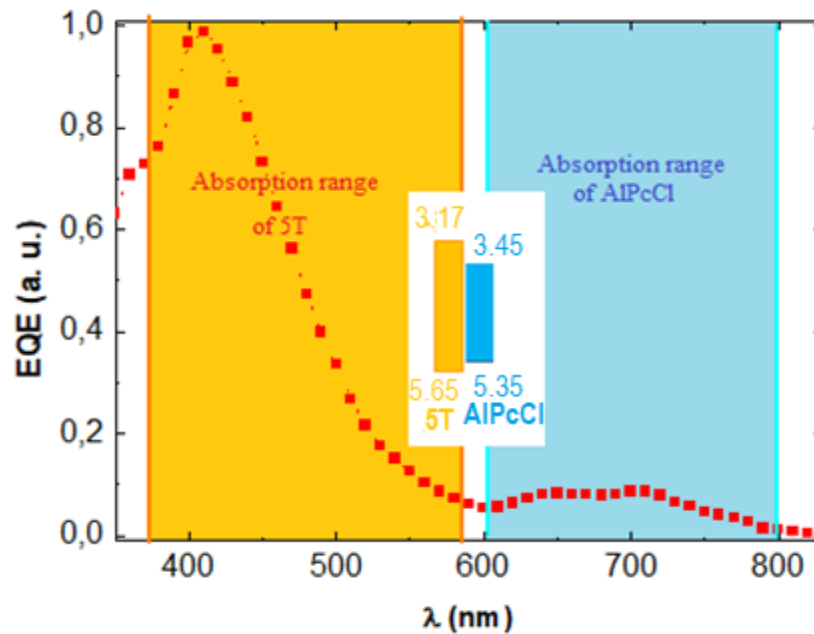


Figure 9. Normalized EQE spectrum of OPV based on 5T/AIPcCl active layer. The absorption ranges of the 5T and AIPcCl molecules are represented schematically as a colored background image.

Inset Fig. 9. Energy band structure of the binary heterojunction 5T/AIPcCl.

1
2
3
4 The absorption range of each molecule is symbolized by the color of the layer obtained with the
5 corresponding molecules: blue for AlPcCl and orange for 5T (see also Fig. 2i). It is clear that the
6 contribution to the photocurrent of AlPcCl is nearly null. It is due to the fact that, as shown by the
7 Fig. 1i (and recalled by the inset of Fig. 9), the energy band configuration, $\Delta(\text{HOMO}_{\text{DA}}-\text{HOMO}_{\text{D}})$
8 < 0 , is opposed to the passage of holes from AlPcCl to 5T, which impedes the collection of hole
9 issued from the excitons created in the AlPcCl layer.
10
11
12
13
14

15 16 **4. Discussion**

17
18 Thus, we scanned all possible configurations of energy band structures, using molecules whose
19 mobility of electric carriers and whose geometry were different. This allows us to set out some
20 general rules to be respected in order to hope to achieve efficient ternary PHT-OPVs. Some were
21 expected, some were not. As shown by the study of ternary cells using pentacene as D, but also
22 ternary cells based on BSTV/SubPc/C₆₀, and the set of studied combinations, the Voc value
23 increases with the energy difference between LUMO_A and HOMO_D, except when the D layer is
24 too rough which drastically decreases the value of Voc, as shown by the results obtained with 5T
25 which RMS is 18 nm. As expected, the hole mobility of the D M8-1 and the electron mobility of
26 the DA MD2 being very small, the results obtained with the OPVs using these molecules, are
27 quite poor, but their general behavior, Voc value, activity of their interfaces with the other
28 molecules included in the cells, are those expected. The results obtained with the 5T/AlPcCl/C₆₀
29 are bad, which confirms that structure with energy band alignment not in accordance with the
30 cascade energy levels configuration cannot give performing OPV. On the other hand, the study of
31 the ternary OPVs using CuPc as donor shows that, if good band matching is necessary to obtain
32 good performances, it is not sufficient. Actually the absence of transfer of energy by FRET in
33 these OPVs results in disappointing efficiency. Moreover, more unexpected, the study of OPVs
34 using CuPc as D shows that the effect of the molecules geometry on the interfaces properties thus
35 realized must not be neglected. When three-dimensional molecules are deposited on plane
36 molecules regularly oriented (parallel or perpendicular to the substrate) it follows a large disorder
37 at the interface which leads to high losses by recombination of carriers, as shown by the failure to
38 obtain saturation current for J_{ph}. This result, even if the context is different, is not without
39 recalling, those concerning ternary BHJ-OPVs where it has been shown that there too, the quality
40 of BHJ depends heavily on the geometry of molecules introduced [12].
41
42
43
44
45
46
47
48
49
50
51
52
53
54
55
56
57
58
59
60
61
62
63
64
65

1
2
3
4 As said above, the review of the results obtained in this study confirms that the V_{oc} value
5 depends directly on the energy difference between the acceptor's LUMO and the donor's
6 HOMO. In the case of quality interface, qV_{oc} may be very close to the difference
7 $\Delta(LUMO_A-HOMO_D)$. However, this value, if it is decisive for the maximum value of V_{oc} , is not
8 the only parameter determining when to its value. The surface roughness of the bottom organic
9 layer of the structure is also decisive. Too high surface roughness dramatically decreases V_{oc}
10 value. The highest V_{oc} value achieved during this work, was obtained from a structure of which
11 D and DA have same HOMO, which avoids the inevitable decrease in the case of stair energy
12 band structure. If a good energy band structure alignment allows to obtain a large V_{oc} value, this
13 of course, is not enough to ensure a high efficiency of the OPV, still it is necessary that the
14 mobility of the carriers of the active layers is sufficient to avoid space charge accumulation that
15 distort the J-V characteristics which results in a S-shaped curve and/or small J_{sc} and FF. On the
16 other hand, if experience shows that the use of a ternary structure in which D and DA or DA and
17 A have the same HOMO is a good starting point to obtain a performing ternary cell, it remains,
18 that in addition to sufficient charge carriers mobility, it is desirable that, besides conventional
19 charge carrier transfer, via the formation of the exciton then the separation of charges at the level
20 of an interface, there be an efficient transfer of energy by FRET.

21 FRET energy transfer results in a migration route which consists in two-step exciton dissociation:
22 diffusion from the donor to the acceptor by Förster resonance energy transfer-FRET, over long
23 length scales, then dissociation.

24 We have shown that ternary OPVs with higher efficiency than that obtained with corresponding
25 binary OPVs fulfill the requirements for effective FRET energy transfer, *i.e.*, a significant
26 overlapping between the PL spectrum of D and the absorption spectrum of DA. When all these
27 requirements are fulfilled, good energy band structure configuration, sufficient charge carriers
28 mobility, complementary light absorption domains, overlapping of PL and light absorption, we
29 have shown that there is still an additional requirement to fulfill, the quality of the interfaces must
30 not be perturbed by incompatible geometry of the molecules. When all these requirements are
31 fulfilled, significant efficiency improvement of ternary OPVs by comparison with corresponding
32 binary OPVs. For instance efficiency of the Pentacene/SubPc/ C_{60} ternary OPV, by comparison
33 with SubPc/ C_{60} is improved by 10%, while that of BSTV/SubPc/ C_{60} is improved by 20%.

5. Conclusion

From this compilation of experimental results a number of rules can be drawn up to be respected if we want to have all the chances of success in the manufacture of ternary cells

-An increase in the RMS induces two opposite effects, one corresponds to an increase of J_{sc} through the increase of the D/A interface area and the second induces leakage currents and therefore Voc and FF deterioration. Therefore it is necessary to look for the RMS which allows to find the optimum trade-off between these opposite influences.

-When the roughness of the organic layers is less than 5 nm, which is generally the case, the difference between the theoretical maximum value of Voc and the experimental value is small, even less than 0.2, which makes it much lower than measured for BHJ-OPVs.

-The mobility of the carriers, electrons and holes, must be at least 10^{-4} cm²/v/s and not too different from each other to obtain a homogeneous charge distribution, this especially in the case of the central layer which, of course, must be ambipolar with balanced electron and hole mobilities.

- In addition to the classical process of charge carrier transfer via light absorption, the creation of the exciton, the migration of the exciton to an interface and the separation of charges at that interface, the possibility of energy transfer by FRET must be effective.

-It appears that, beyond the properties of energy band structures, mobility... the geometry of molecules, planar or not, plays a significant role in obtaining high-performance PHJ-OPVs.

As a conclusion it can be said that, using three of organic molecules with suitable properties, *i.e.* complementary light absorption, not too different carrier's mobility, appropriate energy band structure alignment and also compatible molecule morphologies, it is possible to overpass significantly the binary PHJ-OPV efficiency using ternary PHJ-OPV based on the same molecules, for instance the ternary PHJ-OPV based on the active layer BSTV/SubPc/C₆₀, allows to overpass by 20% the efficiency of corresponding binary OPVs such as SubPc/C₆₀.

Supporting Information

Supporting Information is available from the Wiley Online Library.

Acknowledgements: The authors acknowledge funding from the European Community ERANETMED_ENERG-11-196

Conflicts of interest

There is no conflict of interest to declare.

References

[1] Osbel Almora, Derya Baran, Guillermo C. Bazan, Christian Berger, Carlos I. Cabrera, Kylie R. Catchpole, Sule Erten-Ela, Fei Guo, Jens Hauch, Anita W. Y. Ho-Baillie, T. Jesper Jacobsson, Rene A. J. Janssen, Thomas Kirchartz, Nikos Kopidakis, Yongfang Li, Maria A. Loi, Richard R. Lunt, Xavier Mathew, Michael D. McGehee, Jie Min, David B. Mitzi, Mohammad K. Nazeeruddin, Jenny Nelson, Ana F. Nogueira, Ulrich W. Paetzold, Nam-Gyu Park, Barry P. Rand, Uwe Rau, Henry J. Snaith, Eva Unger, Lídice Vaillant-Roca, Hin-Lap Yip, and Christoph J. Brabec, Device Performance of Emerging Photovoltaic Materials, *Adv. Energy Mater.* 2020; 2002774, DOI: 10.1002/aenm.202002774.

[2] E. Ravishankar, R. E. Booth, C. Saravitz, H. Sederoff, H. W. Ade, B. T. O'Connor, Achieving Net Zero Energy Greenhouses by Integrating Semitransparent Organic Solar Cells, *Joule* 2020; 4: 490–506, doi.org/10.1016/j.joule.2019.12.018

[3] C. Lorch, R. Barnajee, J. Dieterle, A. Hinderhofer, A. Gerlach, J. Drnec, F. Schreiber, Templating effects of a-sexithiophene in donor-acceptor organic thin films, *J. Phys. Chem. C* 2015; 119: 23211-23220, DOI: 10.1021/acs.jpcc.5b06064

[4] J. C. Bernède, Organic photovoltaic cells: History, principle and techniques. *Journal of the Chilean Chemical Society* 2008; 53: 1549-1564, DOI: 10.4067/S0717-97072008000300001

[5] Feng Gao, A New Acceptor for Highly Efficient Organic Solar Cells, *Joule* 2019; 3: 908–919, doi.org/10.1016/j.joule.2019.03.027

[6] Guangye Zhang, Jingbo Zhao, Philip C. Y. Chow, Kui Jiang, Jianquan Zhang, Zonglong Zhu, Jie Zhang, Fei Huang, He Yan, Nonfullerene Acceptor Molecules for Bulk Heterojunction Organic Solar Cells, *Chem. Rev.* 2018; 118: 3447–3507, DOI: 10.1021/acs.chemrev.7b00535

[7] Qishi Liua, Yufan Jianga, Ke Jina, Jianqiang Qina, Jingui Xua, Wenting Lia, Ji Xionga, Jinfeng Liua, Zuo Xiaoa, Kuan Sund, Shangfeng Yangb, Xiaotao Zhangc, Liming Dinga, 18% efficiency organic solar cells, *Science Communications*, 2020; doi.org/10.1016/j.scib.2020.01.001

[8] Kai Wang, Xin Song, Xiao Guo, Yunhao Wang, Xue Lai, Fei Meng, Mengzhen Du, Dongyu Fan, Ren Zhang, Gongqiang Li, Aung Ko Ko Kyaw, Jianpu Wang, Wei Huang and Derya Baran, Efficient as-cast thick film small-molecule organic solar cell with less fluorination on the donor, *Mater. Chem. Front.*, 2020; 4: 206, DOI: 10.1039/c9qm00605b

[9] Xiaodong He, Lunxiang Yin and Yanqin Li, Design of organic small molecules for photovoltaic application with high open-circuit voltage (V_{oc}), *J. Mater. Chem. C*, 2019; 7: 2487, DOI: 10.1039/c8tc06589f

[10] Qian Zhang, Bin Kan, Feng Liu, Guankui Long, Xiangjian Wan, Xiaoqing Chen, Yi Zuo, Wang Ni, Huijing Zhang, Miaomiao Li, Zhicheng Hu, Fei Huang, Yong Cao, Ziqi Liang, Mingtao

1
2
3
4 Zhang, Thomas P. Russell and Yongsheng Chen, Small-molecule solar cells with efficiency over
5 9%, Nature Photonics 2014; DOI: 10.1038/NPHOTON.2014.269
6

7
8 [11] Po R, Roncali J Beyond efficiency: scalability of molecular donor materials for organic
9 photovoltaics. Mater Chem C 2016; 4: 3677–3685, <https://doi.org/10.1039/c5tc03740a>
10

11 [12] Qiaoshi An, Junwei Wang, Xiaoling Ma, Jinhua Gao, Zhenghao Hu, Bin Liu, Huiliang Sun,
12 Xugang Guo, Xiaoli Zhang, Fujun Zhang, Two compatible polymer donors contribute
13 synergistically for ternary organic solar cells with 17.53% efficiency, Energy Environ. Sci., 2020;
14 DOI: 10.1039/d0ee02516j
15
16

17
18 [13] M. Makha, P. Testa, S. B. Anantharaman, J. Heier, S. Jenatsch, N. Leclaire, J.-N. Tisserant, A.
19 C.Véron, Lei Wang, F. Nüesch, R. Hany, Ternary semitransparent organic solar cells with
20 alaminated top electrode, Sci. Technol. Adv. Mater. 2017; 18: 69-75,
21 doi.org/10.1080/14686996.2016.1261602
22
23

24 [14] Kyohei Nakano, Kaori Suzuki, Yujiao Chen, Keisuke Tajima, Roles of Energy/Charge
25 Cascades and Intermixed Layers at Donor/Acceptor Interfaces in Organic Solar Cells, Nature,
26 Scientific Reports 2016; DOI: 10.1038/srep29529
27
28

29 [15] Xiong Gong, Minghong Tong, Fulvio G. Brunetti, Junghwa Seo, Yanming Sun, Daniel
30 Moses, Fred Wudl, Alan J. Heeger, Bulk Heterojunction Solar Cells with Large Open-Circuit
31 Voltage: Electron Transfer with Small Donor-Acceptor Energy Offset, Adv. Mater. 2011; 23:
32 2272–2277, DOI: 10.1002/adma.201003768.
33
34
35

36 [16] D. Baran, T. Kirchartz, S. Wheeler, S. Dimitrov, M. Abdelsamie, J. Gorman, R. S. Ashraf, S.
37 Holliday, A. Wadsworth, N. Gasparini, P. Kaienburg, H. Yan, A. Amassian, C. J. Brabec, J. R.
38 Durrant and I. McCulloch, Reduced voltage losses yield 10% efficient fullerene free organic solar
39 cells with >1 V open circuit voltages, Energy Environ. Sci., 2016; 9: 3783, DOI:
40 10.1039/c6ee02598f.
41
42
43
44

45 [17] Haijun Bin, Zhi-Guo Zhang, Liang Gao, Shanshan Chen, Lian Zhong, Lingwei Xue,
46 Changduk Yang, Yongfang Li J. Am. Chem. Soc. 2016; 138: 4657–4664, DOI:
47 10.1021/jacs.6b01744
48
49

50 [18] Xunfan Liao, Yongjie Cui, Xueliang Shi, Zhaoyang Yao, Heng Zhao, Yongkang An, Peipei
51 Zhu, Yaxiao Guo, Xiang Fei, Lijian Zuo, Ke Gao, Francis Lin, Qian Xie, Lie Chen, Wei Ma,
52 Yiwang Chen, Alex K.-Y. Jen, The role of dipole moment in two fused-ring electron acceptor and
53 one polymer donor based ternary organic solar cells, Mater. Chem. Front., 2020; 4: 1507, DOI:
54 10.1039/d0qm00016g
55
56
57
58
59
60
61
62
63
64
65

1
2
3
4 [19] Desheng Liu, Pu Fan, Dayong Zhang, Xiaohua Zhang, Junsheng Yu, Förster resonance energy
5 transfer and improved charge mobility for high performance and low-cost ternary polymer solar
6 cells, *Solar Energy* 2019; 189: 186–193, doi.org/10.1016/j.solener.2019.07.060
7
8

9
10 [20] D. C. Coffey, A. J. Ferguson, N. Kopidakis, G. Rumbles, Photovoltaic charge generation in
11 organic semiconductors based on long-range energy transfer. *ACS NANO* 2010; 4: 5437–5445,
12 doi.org/10.1021/nn101106b
13

14
15 [21] An Q, Zhang F, Zhang J, Tang W, Deng Z, Hu B, Versatile ternary organic solar cells: a
16 critical review. *Energy Environ Sci.* 2016; 9: 281–322, doi.org/10.1039/C5EE02641E
17

18
19 [22] <https://www.heliatek.com/product/>
20

21 [23] Zhenzhen Zhang and Yuze Lin, Organic Semiconductors for Vacuum-Deposited Planar
22 Heterojunction Solar Cells, *ACS Omega* 2020; 5: 24994–24999,
23 doi.org/10.1021/acsomega.0c03868
24

25
26 [24] Z. El Jouad, L. Cattin, F. Martinez, G. Neculqueo, G. Louarn, M. Addou, P. Predeep, J.
27 Manuvel, J. C. Bernède, Improvement of pentathiophene/fullerene planar heterojunction
28 photovoltaic cells by improving the organic films morphology through the anode buffer bilayer.
29 *Eur Phys J Appl Phys.* 2016; 74: 24603, doi.org/10.1051/epjap/2015150335
30
31

32
33 [25] F. Martinez, G. Neculqueo, J. C. Bernède, L. Cattin, M. Makha, Influence of the presence of
34 Ca in the cathode buffer layer on the performance and stability of organic photovoltaic cells using a
35 branched sexithienylenevinylene oligomer as electron donor. *Phys Status Solidi A* 2015;
36 212:1767–1773, doi.org/10.1002/pssa.201431845
37
38

39
40 [26] E. Ortega, R. Montecinos, L. Cattin, F.R. Díaz, M.A. del Valle, J.C. Bernède, Synthesis,
41 characterization and photophysical-theoretical analysis of compounds A- π -D. 1. Effect of
42 alkyl-phenyl substituted amines in photophysical properties, *Journal of Molecular Structure* 2017;
43 1141: 615-623, doi.org/10.1016/j.molstruc.2017.04.019
44
45

46
47 [27] J. Grolleau, F. Gohier, M. Allain, S. Legoupy, C. Cabanetos, P. Frère, Syntheses via a direct
48 arylation method of push–pull molecules based on triphenylamine and
49 3-cyano-4-hexyloxythiophene moieties, *Org. Electron.* 2017; 42: 322–328,
50 doi.org/10.1039/C6OB02036D
51
52

53
54 [28] Yongshuai Gong, Yiman Dong, Biao Zhao, Runnan Yu, Siqian Hu, Zhan'ao Tan, Diverse
55 applications of MoO₃ for high performance organic photovoltaics: fundamentals, processes and
56 optimization strategies, *J. Mater. Chem. A*, 2020; 8: 978, DOI: 10.1039/c9ta12005j
57

58
59 [29] Y. Lare, B. Kouskoussa, K. Benchouk, S. O. Djobo, L. Cattin, F. R. Diaz, M. Gacitua, T.
60 Abachi, M. A. del Valle, F. Amijo, G. A. East, J. C. Bernède, Influence of the exciton blocking
61
62
63
64
65

1
2
3
4 layer on the stability of layered organic solar cells, *J Phys. Chem. Solids* 2011; 72: 97–103,
5 doi:10.1016/j.jpcs.2010.11.006
6

7
8 [30] B. Ebenhoch, N. B. A. Prasetya, V. M. Rotello, G. Cooke, I. D. W. Samuel,
9 Solution-processed boron subphthalocyanine derivatives as acceptors for organic
10 bulk-heterojunction solar cells, *J. Mater. Chem. A*, 2015; 3: 7345-7352,
11 doi.org/10.1039/C5TA00715A
12

13
14 [31] N. Beaumont, S.W. Cho, P. Sullivan, D. Newby, K.E. Smith, T.S. Jones, Boron
15 subphthalocyanine chloride as an electron acceptor for high-voltage fullerene-free organic
16 photovoltaics. *Adv. Funct. Mater.* 2012; 22: 561, doi.org/10.1002/adfm.201101782
17

18
19 [32] L. Cattin¹, J. C. Bernède, Y. Lare, S. Dabos-Seignon, N. Stephant, M. Morsli, P. P. Zamora, F.
20 R. Diaz, M. A. del Valle, Improved performance of organic solar cells by growth optimization of
21 MoO₃/CuI double-anode buffer, *Phys. Status Solidi A* 2013; 210: 802–808; DOI
22 10.1002/pssa.201228665
23

24
25 [33] Wei Chen, Han Huang, Shi Chen, Yu Li Huang, Xing Yu Gao, and Andrew Thye Shen Wee,
26 Molecular Orientation-Dependent Ionization Potential of Organic Thin Films, *Chem. Mater.* 2008;
27 20: 7017–7021, Doi: 10.1021/cm8016352
28

29
30 [34] Xin Xiao, J. D. Zimmerman, B. E. Lassiter, K. J. Bergemann, and S. R. Forrest, A hybrid
31 planar-mixed tetraphenylidibenzoperiflanthene/C70 photovoltaic cell, *Appl. Phys. Lett.* 2013; 102:
32 073302, doi: 10.1063/1.4793195
33

34
35 [35] A. J. Pal, J. Paloheimo, H. Stubb, Molecular light-emitting diodes using quinquethiophene
36 Langmuir-Blodgett films. *Appl Phys Lett* 1995; 67: 3909–39011
37

38
39 [36] K. Nakano, K. Tajima, Organic planar heterojunctions: From models for interfaces in bulk
40 heterojunctions to high performance solar cells. *Adv Mater* 2017; 29: 1603269,
41 doi.org/10.1002/adma.201603269
42

43
44 [37] Rhonda F. Salzman, Jiangeng Xue, Barry P. Rand, Alex Alexander, Mark E. Thompson ,
45 Stephen R. Forrest, The effects of copper phthalocyanine purity on organic solar cell performance,
46 *Organic Electronics* 2005; 6: 242–246, doi: 10.1016/j.orgel.2005.09.001
47

48
49 [38] F. Anger, J. O. Ossó, U. Heinemeyer, K. Broch, R. Scholz, A. Gerlach, F. Schreiber,
50 Photoluminescence spectroscopy of pure pentacene, perfluoropentacene, and mixed thin films, *J.*
51 *Chem. Phys.* 2012; 136: 054701, doi:10.1063/1.3677839
52

53
54 [39] D. Frackowiak, A. Planner, A. Waszkowiak, A. Boguta, R-M. Ion, K. Wiktorowicz, Yield of
55 intersystem (singlet–triplet) crossing in phthalocyanines evaluated on the basis of a time in
56 resolved photothermal method, *Journal of Photochemistry and Photobiology A: Chemistry* 2001;
57 141: 101–108,
58
59
60
61
62
63
64
65

- 1
2
3
4 [40] Fei Yan, Wen Lian Li, Bei Chua, Tian Le Li, Wen Ming Su, Zi Sheng Su, Jian Zhuo Zhu,
5 Dong Fang Yang, Guang Zhang, De Feng Bi, and Liang Liang Han, Sensitized
6 electrophosphorescence of infrared emission diode based on copper phthalocyanine by an
7 ytterbium complex, *Appl. Phys. Lett.* 2007; 91: 203512, DOI: 10.1063/1.2811953
8
9
- 10 [41] Chuan-Hui Cheng, Zhao-Qi Fan, Shu-Kun Yu, Wen-Hai Jiang, and Xu Wang Guo-Tong
11 Du, Yu-Chun Chang, and Chun-Yu Ma, 1.1 μm near-infrared electrophosphorescence from
12 organic light-emitting diodes based on copper phthalocyanine, *Appl. Phys. Lett.* 2006; 88: 213505,
13 DOI: 10.1063/1.2206678.
14
15
- 16 [42] Zhen-Giang Guo, Chuan-Hui Cheng, Zhao-Qi Fan, Wei He, Shu-Kun Yu, Yu-Chun Chang,
17 Xi-Guang Du, Xu Wang, Guo-Tong Du, Near-Infrared Emission from Organic Light-Emitting
18 Diodes Based on Copper Phthalocyanine with a Periodically Arranged Alq₃:CuPc/DCM
19 Multilayer Structure, *Chin. Phys. Lett.* 2008; 25: 715
20
21
- 22 [43] Matthew T. Lloyd, Yee-Fun Lim, and George G. Malliaras, Two-step exciton dissociation in
23 poly,*3*-hexylthiophene.../fullerene heterojunctions, *Appl. Phys. Lett.* 2008; 92: 143308, DOI:
24 10.1063/1.2908165.
25
- 26 [44] C. W. Tang, Two-layer organic photovoltaic cell, *Appl. Phys. Lett.* 1986; 48: 183,
27 <https://doi.org/10.1063/1.96937>
28
29
- 30 [45] Z. El Jouad, E.M. El-Menyawy, G. Louarn, L. Arzel, M. Morsli, M. Addou, J. C. Bernède and
31 L. Cattin, The effect of the band structure on the Voc value of ternary planar heterojunction organic
32 solar cells based on pentacene, boron subphthalocyanine chloride and different electron acceptors,
33 *Journal of Physics and Chemistry of Solids* 2020; 136: 109142,
34 doi.org/10.1016/j.jpcs.2019.109142
35
36
- 37 [46] L. Cattin, Z. El Jouad, L. Arzel, G. Neculqueo, M. Morsli, F. Martinez, M. Addou, J.C.
38 Bernède, Comparison of performances of three active layers cascade OPVCs with those obtained
39 from corresponding bi-layers, *Solar Energy* 2018; 171: 621–628,
40 doi.org/10.1016/j.solener.2018.07.008
41
42
- 43 [47] L. Cattin, Z. El Jouad, M. B. Siad, A. Mohammed Krarroubi, G. Neculqueo, L. Arzel, N.
44 Stephant, M. Mastropasqua Talamo, F. Martinez, M. Addou, A. Khelil, M. Morsli, P. Blanchard, J.
45 C. Bernède, Highlighting the possibility of parallel mechanism in planar ternary photovoltaic cells,
46 *AIP ADVANCES* 2018; 8: 115329, doi.org/10.1063/1.5037531
47
48
49
- 50 [48] Kjell Cnops, Barry P. Rand, David Cheyens, Bregt Verreert, Max A. Empl & Paul Heremans,
51 8.4% efficient fullerene-free organic solar cells exploiting long-range exciton energy transfer, *Nat.*
52 *Commun.* 2014; 5: 3406, DOI: 10.1038/ncomms4406.
53
54
- 55 [49] Christopher M. Proctor and Thuc-Quyen Nguyen, Effect of leakage current and shunt
56 resistance on the light intensity dependence of organic solar cells, *Appl. Phys. Lett.* 2015; 106:
57 083301, doi.org/10.1063/1.4913589.
58
59
60
61
62
63
64
65

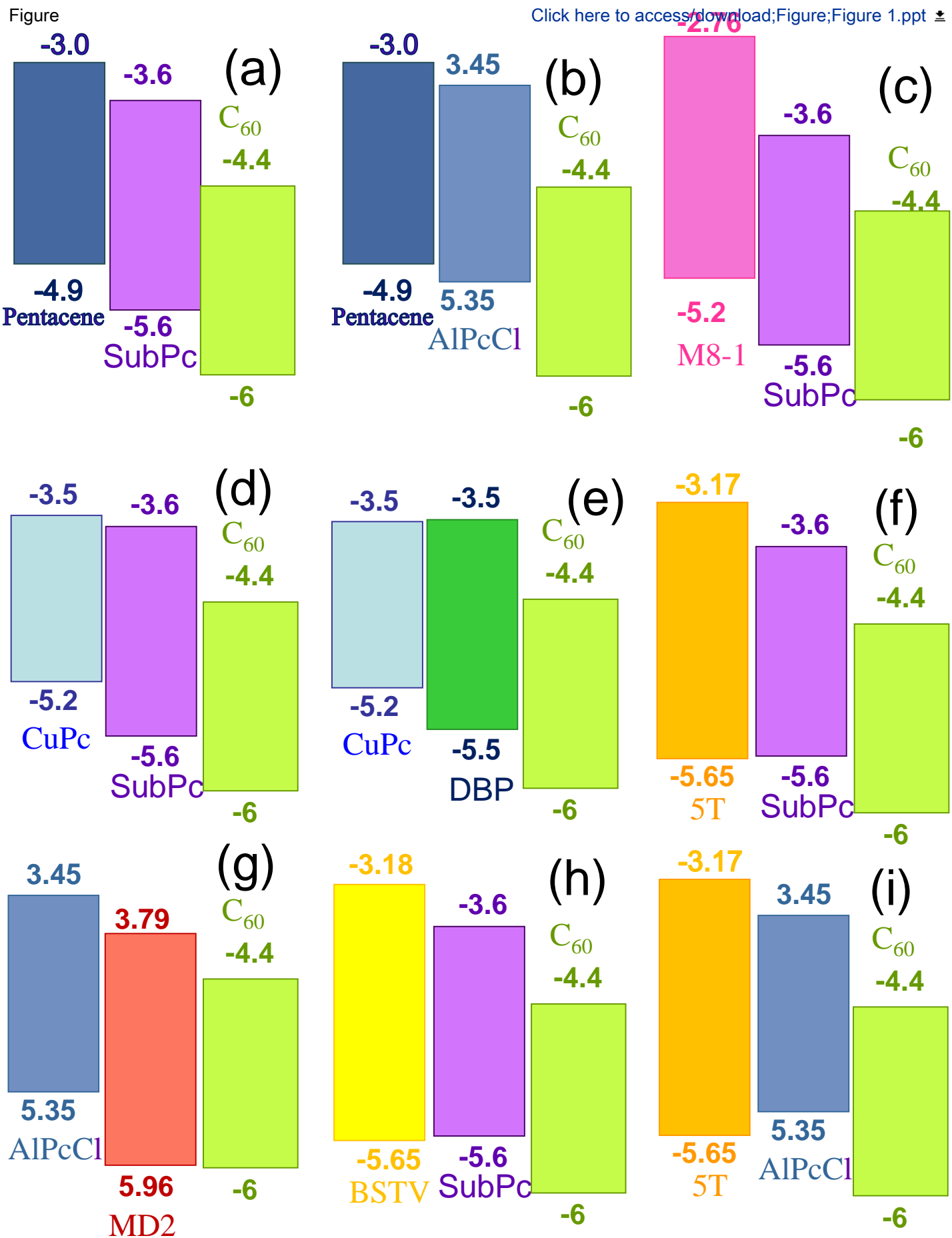
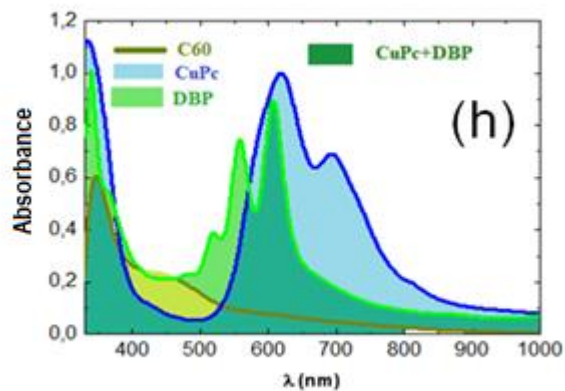
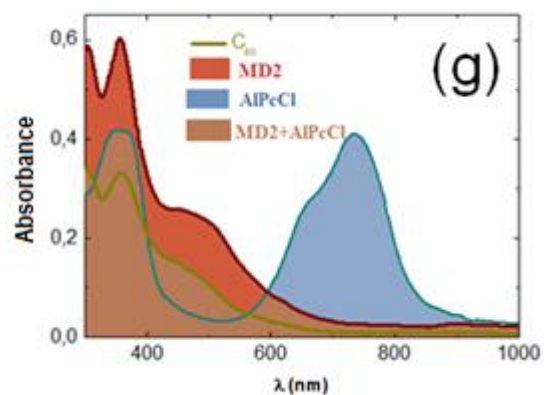
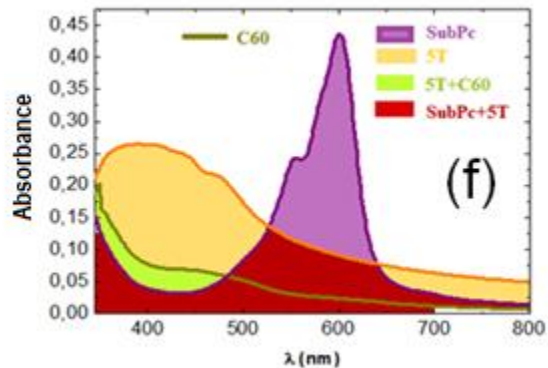
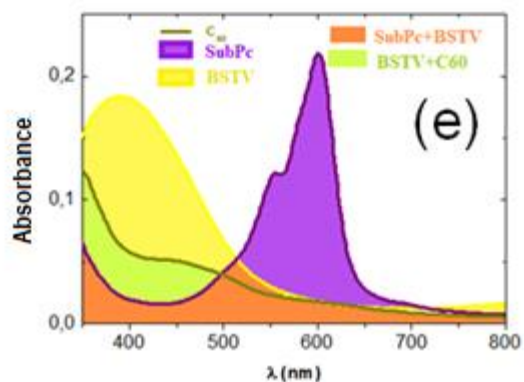
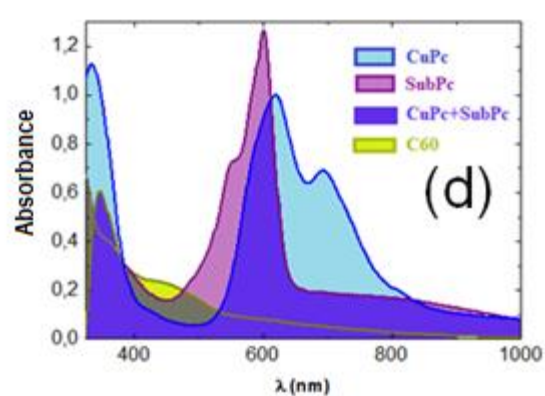
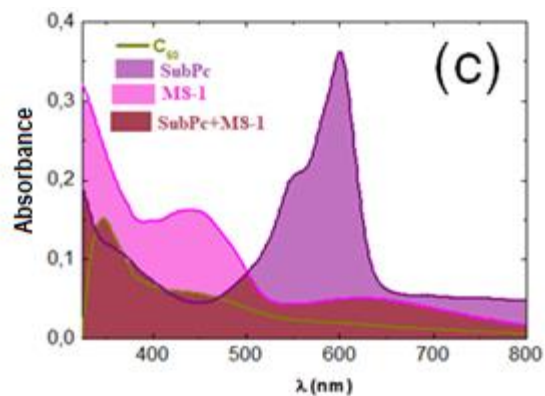
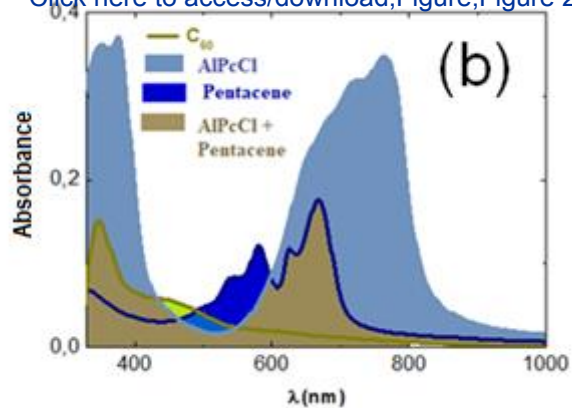
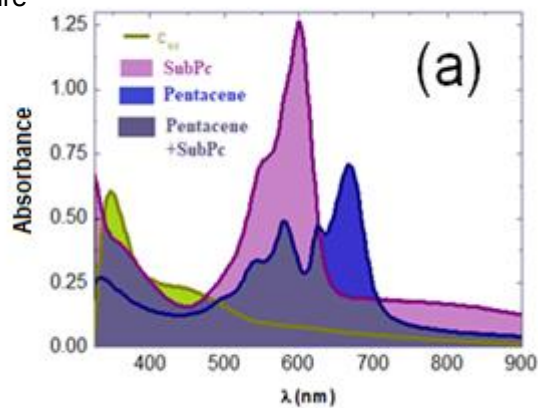


Figure 1.



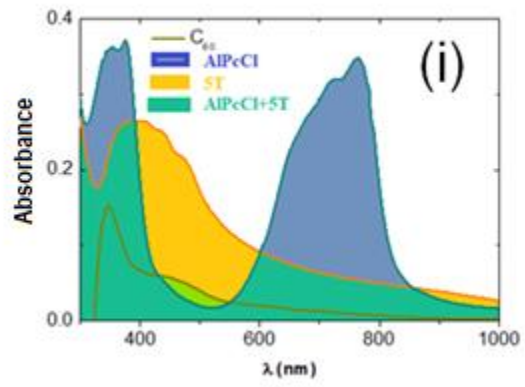


Figure 2

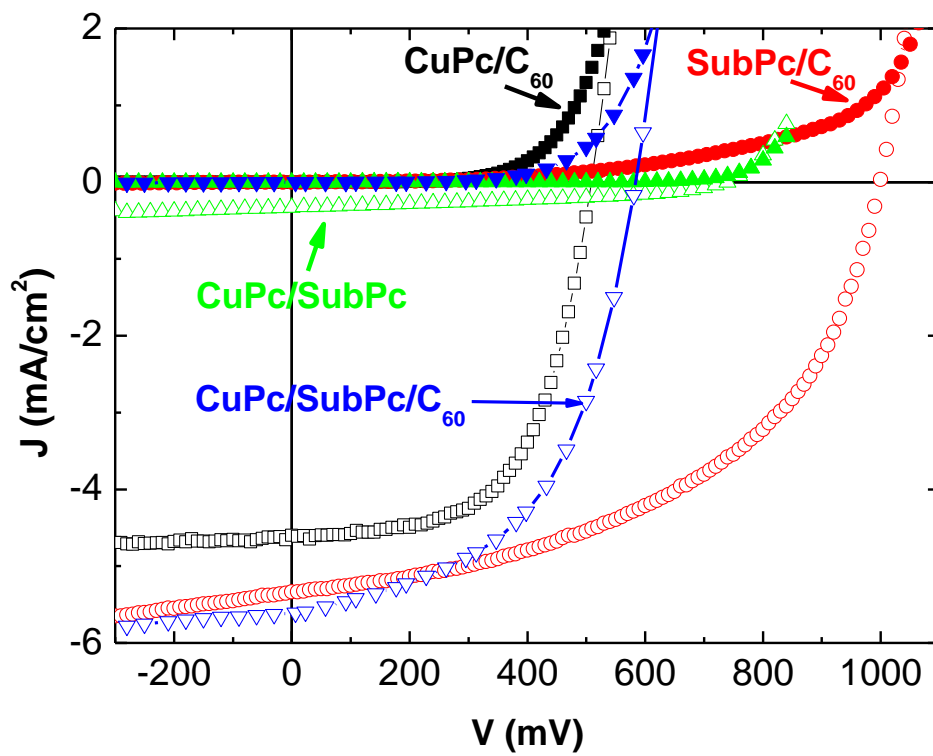


Figure 3.

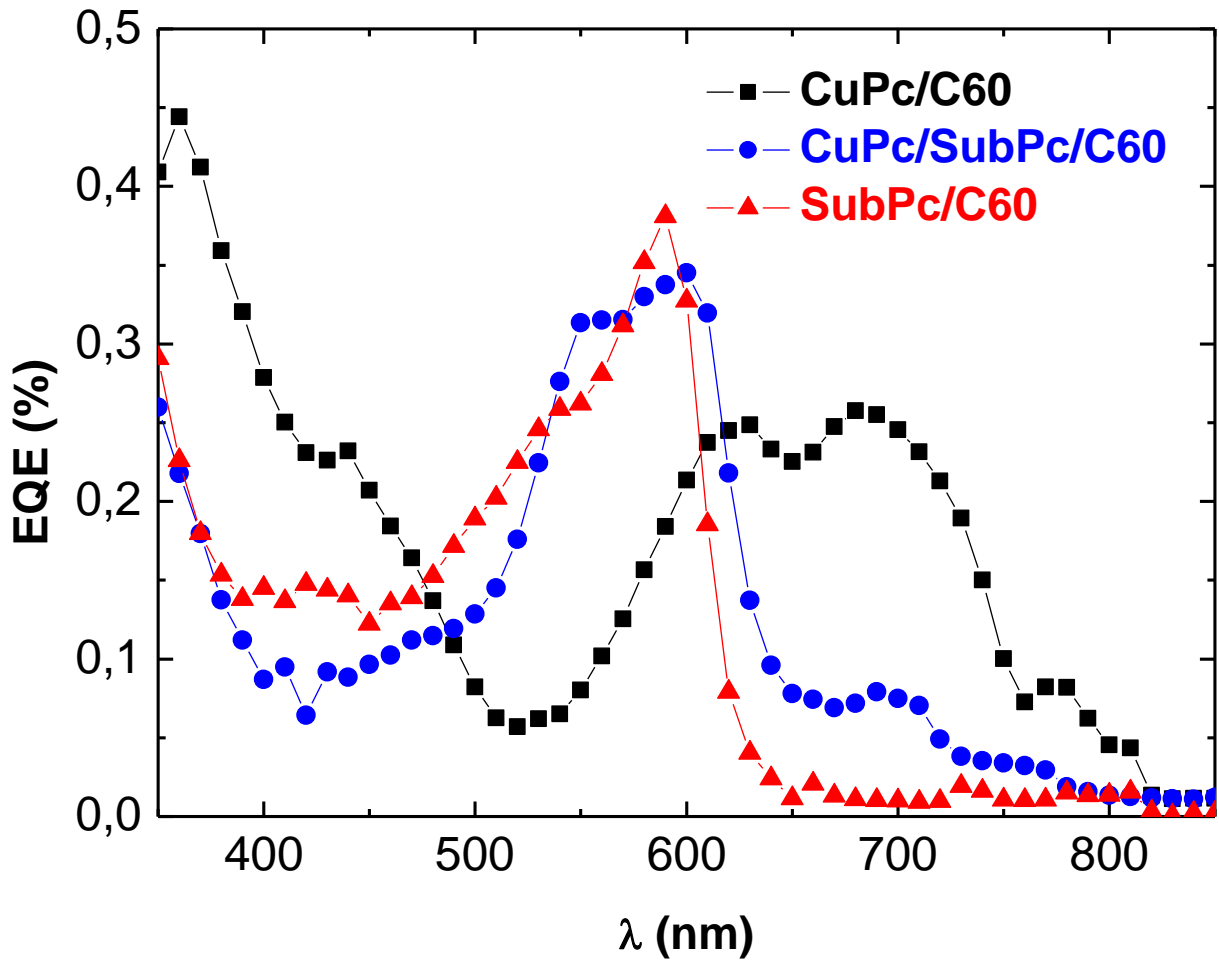


Figure 4.

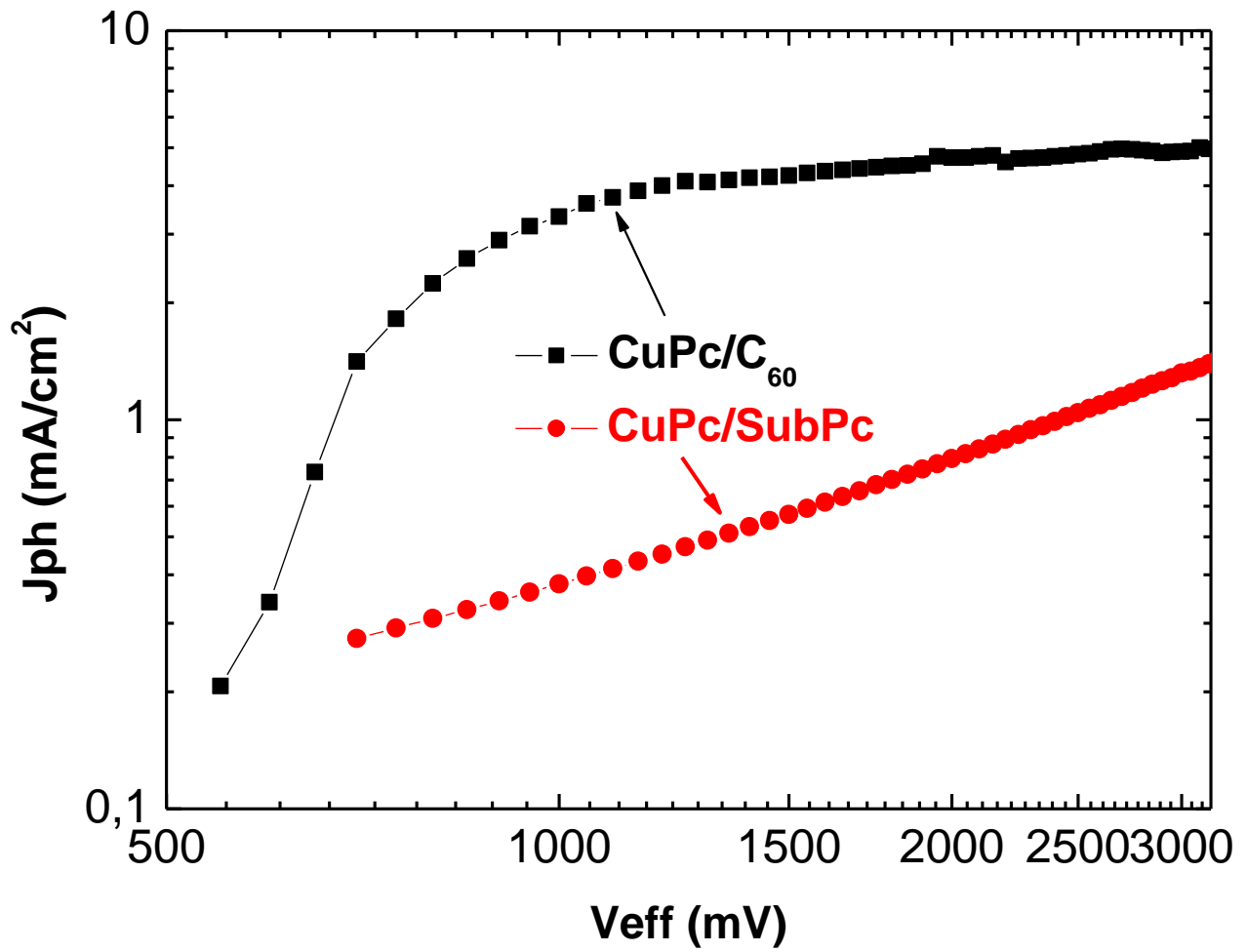


Figure 5.

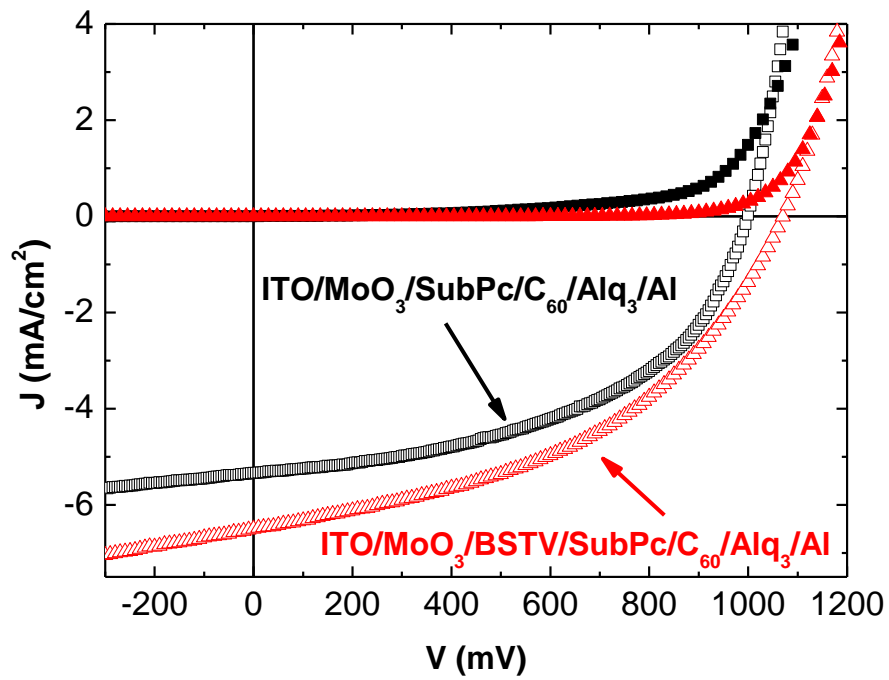


Figure 6.

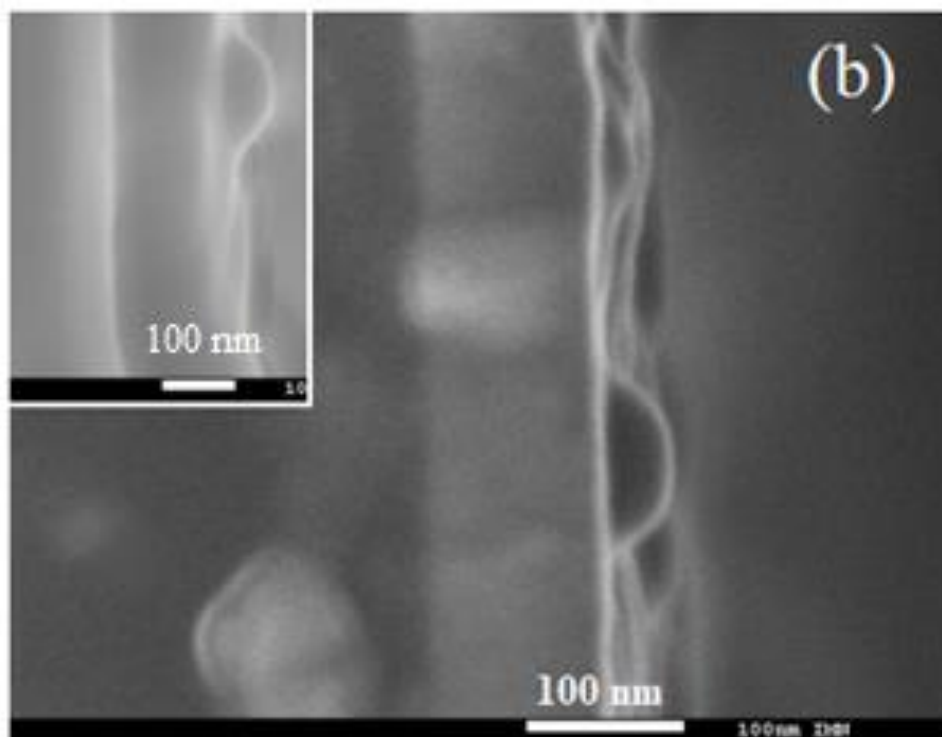
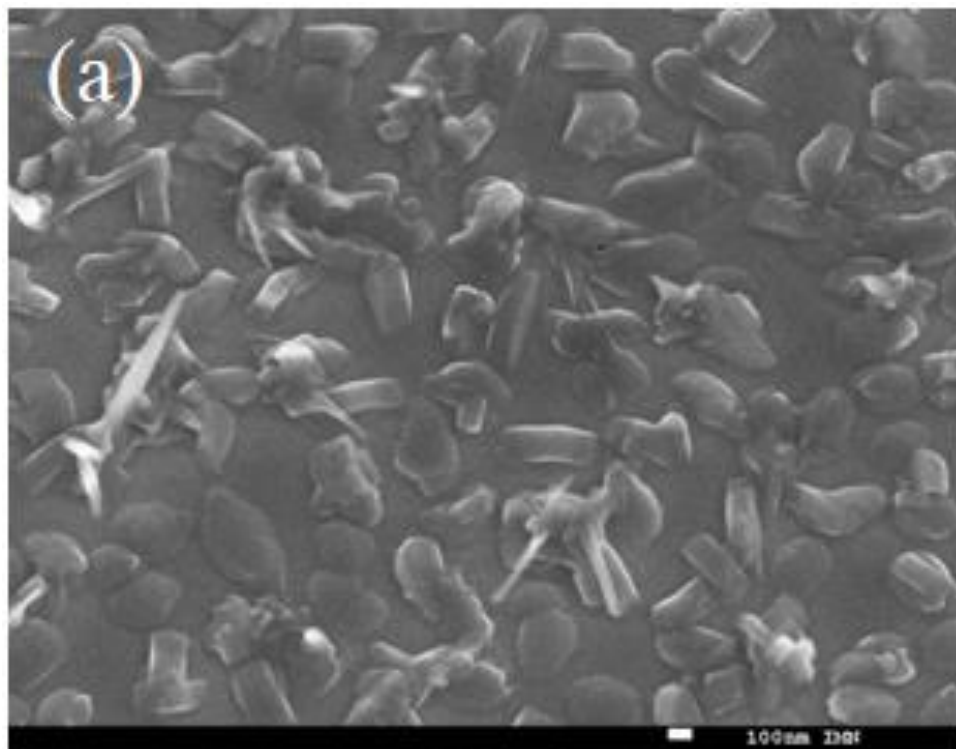


Figure 7.

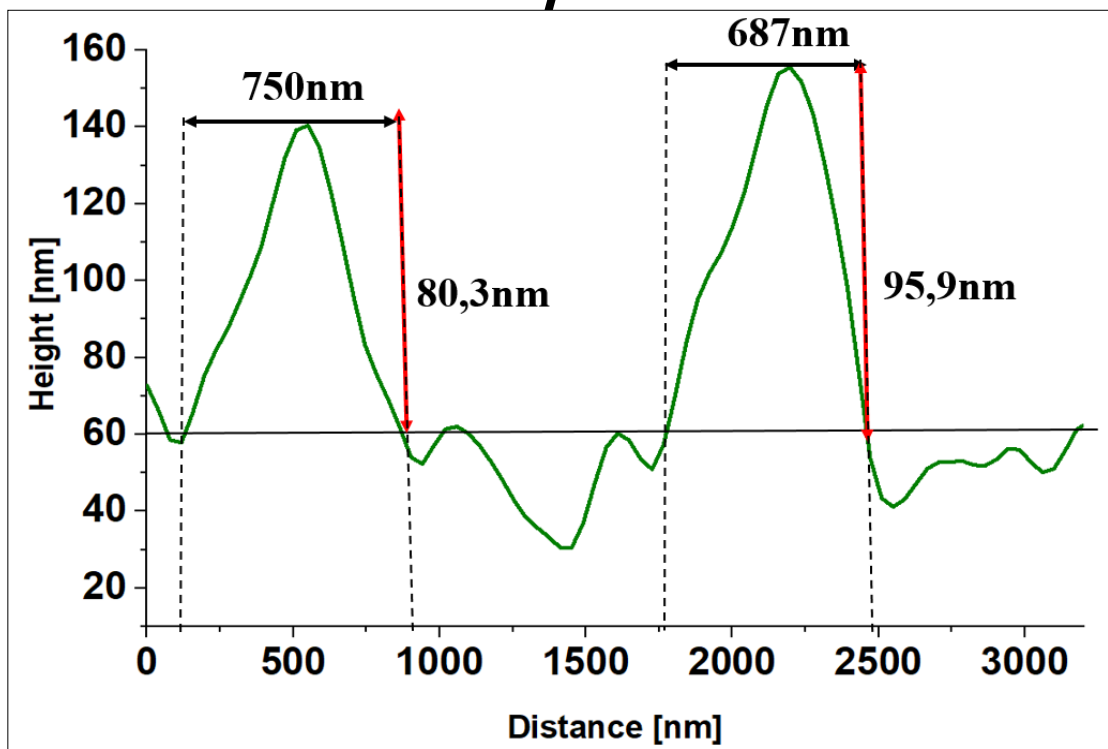
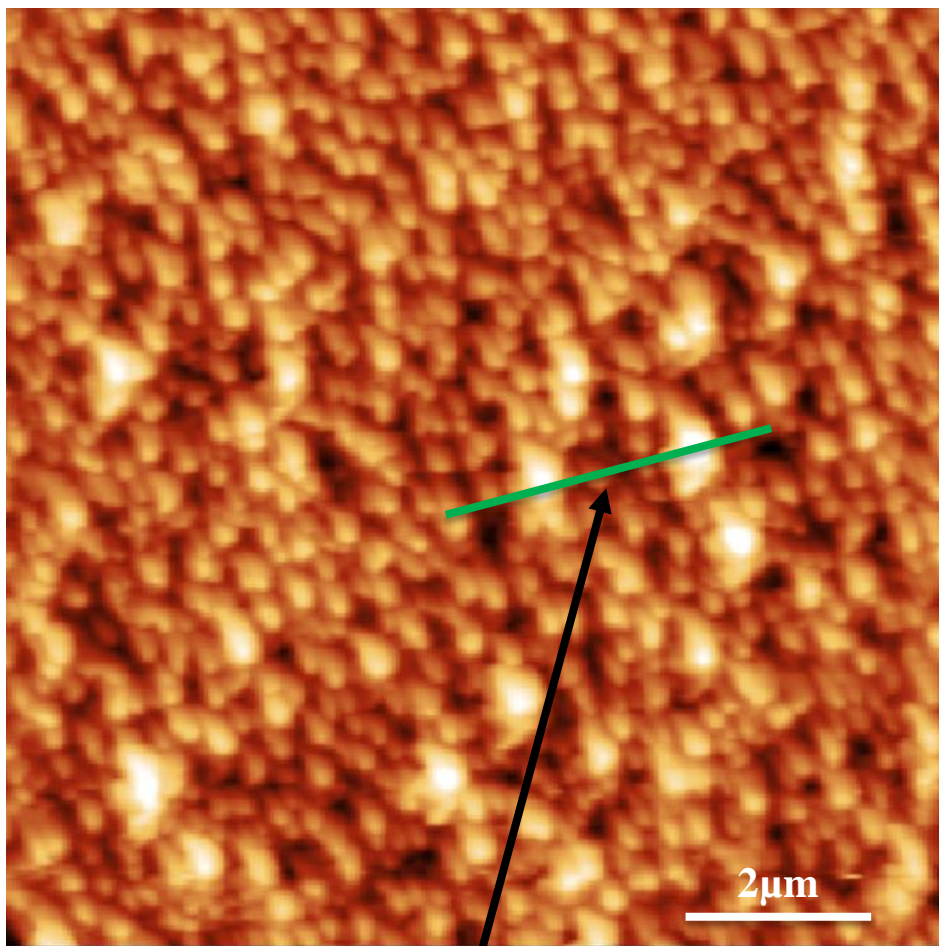


Figure 8

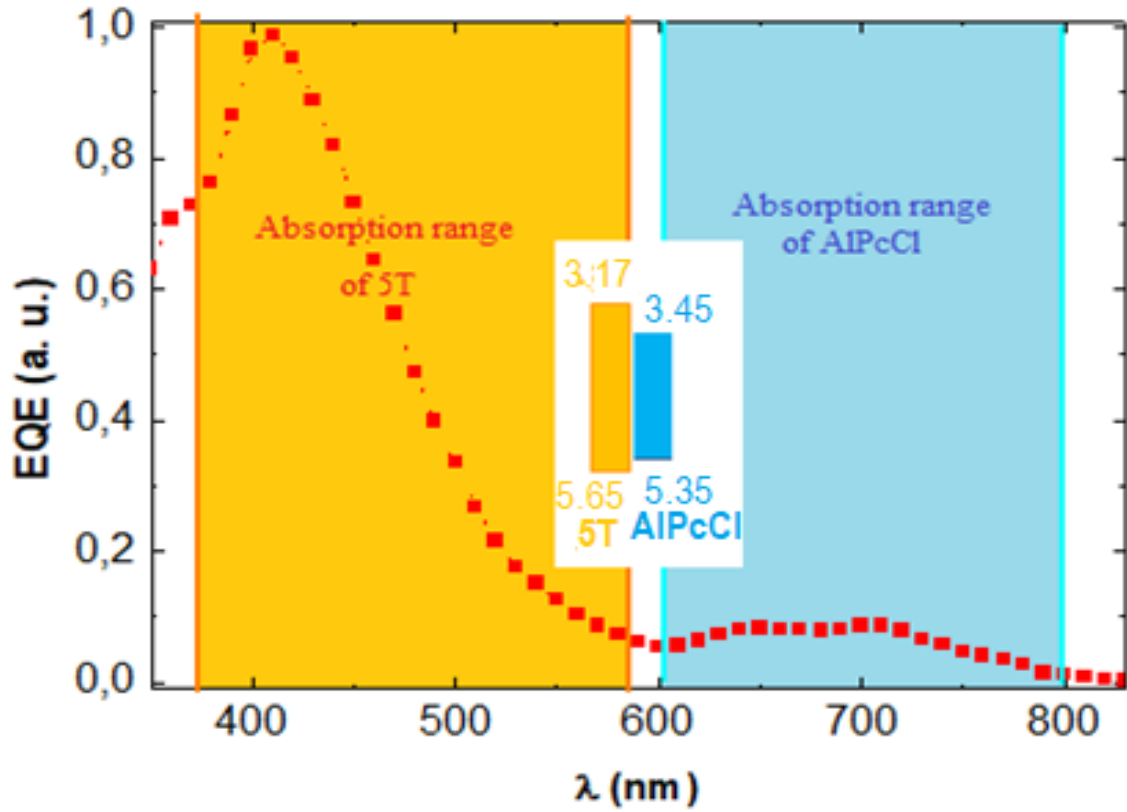


Figure 9.

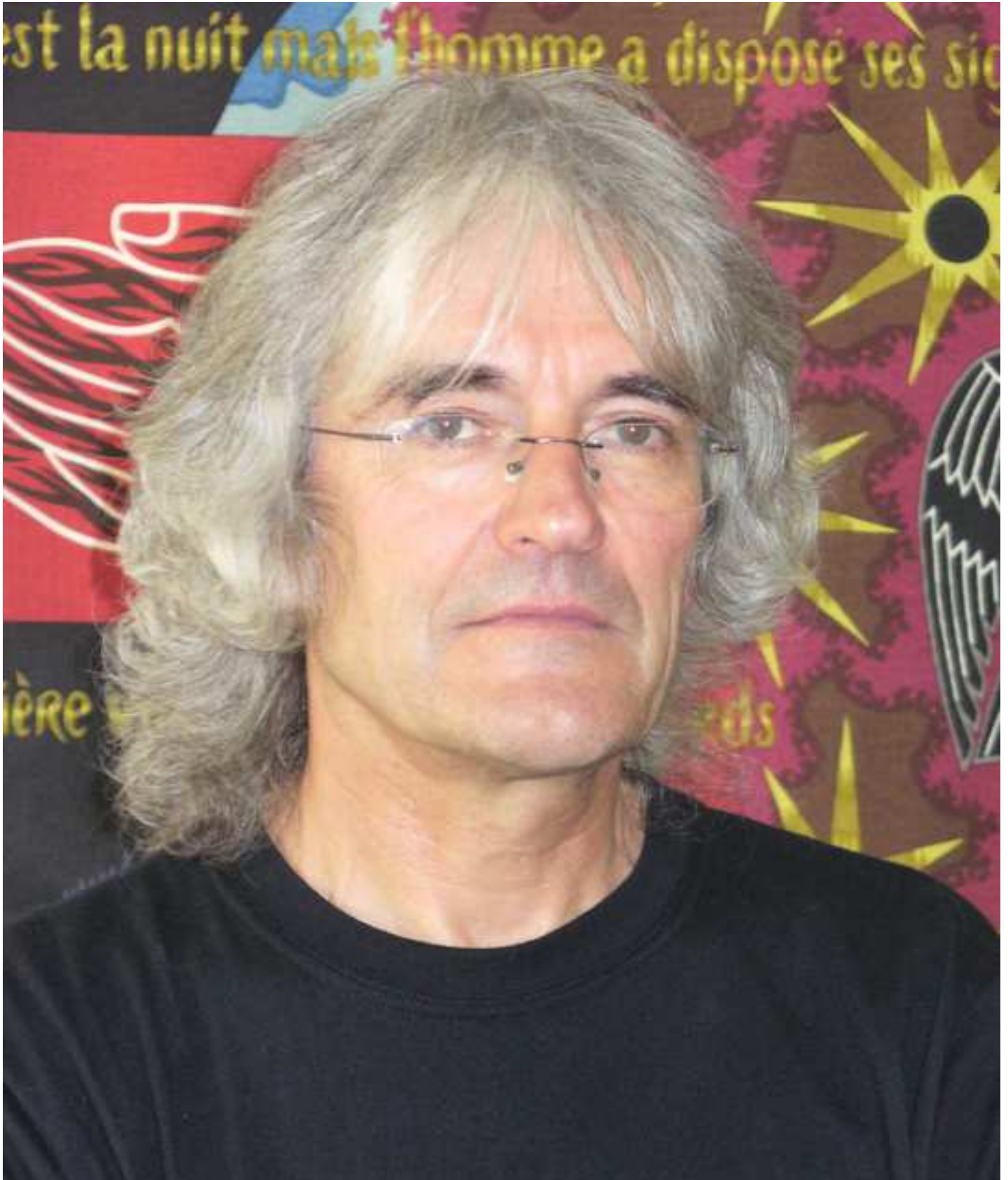
Biography

Jean Christian Bernède, Senior Searcher,

Thèse d'Etat, Université de Nantes, France



After working on the thin layer structures of chalcogenides presenting so-called "Ovshinsky" commutations, he turned to the study of photovoltaic cells in thin layer. Firstly, inorganic cells essentially based on CuInGaSe_2 (CIGS). Later, he turned to organic electroluminescent diodes (OLED) and organic photovoltaic cells (OPV Cells). He was particularly interested in the interfaces electrode/organic material. Subsequently he extended his field of investigation to the transparent conductive layers alternatives to the ITO.



Declaration of interests

The authors declare that they have no known competing financial interests or personal relationships that could have appeared to influence the work reported in this paper.

The authors declare the following financial interests/personal relationships which may be considered as potential competing interests:



Click here to access/download
e-Component
Supporting information.docx



Table 1. Parameters of the OPV family using CuPc, SubPc and C₆₀.

Active layer (thickness-nm)	Voc (V)	Jsc (mA cm ⁻²)	FF (%)	η (%)
CuPc (30)/C ₆₀ (40)	0.50	4.68	60	1.42
SubPc (20)/C ₆₀ (40)	1.00	5.33	50	2.63
CuPc (30)/SubPc (15)	0.74	0.33	41	0.09
CuPc (30)/SubPc (15) ^{a)}	0.75	0.48	33	0.12
CuPc (30)/SubPc (15)/C ₆₀ (40)	0.58	5.54	55	1.77

^{a)} HTL MoO₃/CuI and not MoO₃ alone.

Table 2. Diverse parameters of the organic layers used.

Molecule	μ_{e^-} ($\text{cm}^2 \text{v}^{-1} \text{s}^{-1}$)	μ_{h^+} ($\text{cm}^2 \text{v}^{-1} \text{s}^{-1}$)	RMS ^{b)} (nm)	O. D. Absorption range (nm)	PL ^{c)} Emission range (nm)
Pentacene	-	$7.5 \cdot 10^{-3}$	4-7	500-700	660-700 ; 730-950
CuPc	$5.8 \cdot 10^{-3}$	$1.1 \cdot 10^{-3}$ ^{a)}	3	550-800 ; 300-400	1075-1175
M8-1	$1.6 \cdot 10^{-9}$	$6 \cdot 10^{-7}$	3.5	530-580 ; 300-530	525-750
BSTV	-	$9.5 \cdot 10^{-6}$	1.55	350-500	500-650
5T	-	$1.7 \cdot 10^{-4}$	18	350-600	475-625
AlPcCl	$6.9 \cdot 10^{-4}$	$4 \cdot 10^{-5}$	6	800-600 ; 400-300	660-720 ; (770)
DBP	$1.6 \cdot 10^{-4}$	$2 \cdot 10^{-4}$	-	500-650 ; 300-450	-
SubPc	$8 \cdot 10^{-3}$	$1.7 \cdot 10^{-5}$	-	500-650 ; 430-300	-
MD2	$1.5-3 \cdot 10^{-7}$	$1 \cdot 10^{-5}$	-	500-300	-

^{a)} When deposited onto CuI the hole mobility of CuPc is $2 \cdot 10^{-3} \text{ cm}^2 \text{v}^{-1} \text{s}^{-1}$

^{b)} Values measured for the organic bottom layer D.

^{c)} From luminescence spectra shown in Fig. S7 or extracted from the bibliography: 5T [35], Pentacene [38], AlPcCl [39], and CuPc [40].

Table 3. Parameters of the OPV family using CuPc, DBP and C₆₀.

Active layer (thickness-nm)	Voc (V)	Jsc (mA cm ⁻²)	FF (%)	η (%)
DBP (20)/C ₆₀ (40)	0.76	3.01	38	0.88
CuPc (30)/C ₆₀ (40)	0.50	4.68	60	1.42
CuPc (30)/DBP (15)	0.24	1.02	25	0.06
CuPc (30)/DBP (10)/C ₆₀ (40)	0.30	1.59	40	0.20